phyllosilicates in the Mawrth Vallis region of Mars

D. Loizeau, N. Mangold, F. Poulet, J.-P. Bibring, A. Gendrin, V. Ansan, C. Gomez, B. Gondet, Y. Langevin, Ph. Masson, et al.

Phyllosilicates in the Mawrth Vallis region of Mars

D. Loizeau,[1] N. Mangold,[1] F. Poulet,[2] J.-P. Bibring,[2] A. Gendrin,[2] V. Ansan,[1] C. Gomez,[2] B. Gondet,[2] Y. Langevin,[2] P. Masson,[1] and G. Neukum[3]

Received 5 December 2006; revised 26 March 2007; accepted 13 June 2007; published 27 July 2007.

[1] OMEGA/Mars Express has discovered large outcrops rich in phyllosilicates in the region of Mawrth Vallis, Mars (around 20°W, 25°N). The region is located in Noachian highly cratered terrains, close to the limit of the Martian dichotomy, where the outflow channel Mawrth Vallis cuts the highlands. We have examined this region using OMEGA spectra of the surface from 0.9 μm to 2.6 μm, with spatial sampling from 500 m to 3 km, offering a full coverage of the region. OMEGA spectra show two broad bands centered at 1 μm and 2.2 μm, revealing the presence of clinopyroxene on dark surfaces. Phyllosilicates have been identified by absorption bands at 1.4 μm, 1.9 μm, and 2.2 or 2.3 μm. Comparison with laboratory spectra reveals similarities with Al-OH smectites such as montmorillonites, or Fe- or Mg-OH smectites such as nontronite. A precise location of the phyllosilicate-rich areas on visible HRSC images indicates that they are placed exclusively on bright outcrops, mostly on the plateaus, dated to the Noachian period. On HRSC and MOC images the phyllosilicate-rich outcrops reveal strong erosional features such as numerous residual buttes composed of layers a few meters thick. The phyllosilicate-rich unit corresponds to a geological unit more than 100 m thick, over a horizontal extension approximately of 300 km $\times$ 400 km. This unit implies a large volume of altered rocks, either in situ or after transport and deposition, in Noachian terrains, revealing a different climatic and geologic environment from the present one.

Citation: Loizeau, D., et al. (2007), Phyllosilicates in the Mawrth Vallis region of Mars, *J. Geophys. Res.*, *112*, E08S08, doi:10.1029/2006JE002877.

1. Introduction

[2] The imaging hyper-spectrometer OMEGA (Observatoire pour la Minéralogie, l'Eau, les Glaces et l'Activité) [e.g., *Bibring et al.*, 2004] aboard Mars Express has detected mineralogically diverse phyllosilicates on the surface of Mars [*Poulet et al.*, 2005; *Bibring et al.*, 2006]. One of the major phyllosilicate-rich regions has been found around the Mawrth Vallis outflow channel (about 20°W, 25°N), located west of Arabia Terra at the limit of the Martian dichotomy (Figure 1). Mawrth Vallis cuts plateaus standing between −3300 m and −1500 m in elevation dated to the Noachian period [*Scott and Tanaka*, 1986; *Edgett and Parker*, 1997], before debouching into the eastern side of Chryse Planitia. This region was previously suggested to be composed of primitive outcrops of the Martian crust on the basis of Viking and MOC (Mars Observer Camera) narrow angle images [*Edgett and Parker*, 1997; *Malin and Edgett*, 2000; *Edgett and Malin*, 2002].

[3] In this region, OMEGA has obtained spectra of phyllosilicates similar to smectites such as montmorillonites (Al-OH smectites) and nontronite (Fe-OH smectites) [*Poulet et al.*, 2005]. The presence of phyllosilicates on Mars has many implications for the early history of the planet, because their formation likely required the presence of liquid water, although the exact process of formation is not certain [*Poulet et al.*, 2006]. The detailed study of the geomorphology and thermal properties of the terrains rich in phyllosilicates will give us complementary information for a better understanding of their formation and of the implications for the primitive environment of Mars. The composition and spatial extent of the phyllosilicate mineralogy in the Mawrth Vallis region are shown using OMEGA data sets, while the High Resolution Stereo Camera (HRSC) aboard Mars Express [e.g., *Neukum and Jaumann*, 2004], helps us to study the overall geomorphology of the region, associated with the topography from the Mars Orbiter Laser Altimeter (MOLA) [e.g., *Smith et al.*, 2001], aboard Mars Global Surveyor (MGS). The Mars Orbiter Camera (MOC) [e.g., *Malin et al.*, 1992] aboard MGS and the Thermal Emission Imaging System (THEMIS) [e.g., *Christensen et al.*, 2004] aboard Mars Odyssey provide additional data about the geology and thermophysical properties of the area. In this paper, we first present the use of the different data sets, then the regional mineralogical differences that

[1] Laboratoire IDES, Université Paris XI, Orsay, France.
[2] Institut d'Astrophysique Spatiale, Université Paris XI, Orsay, France.
[3] Institut für Geologische Wissenschaften, Freie Universität Berlin, Berlin, Germany.

0148-0227/07/2006JE002877

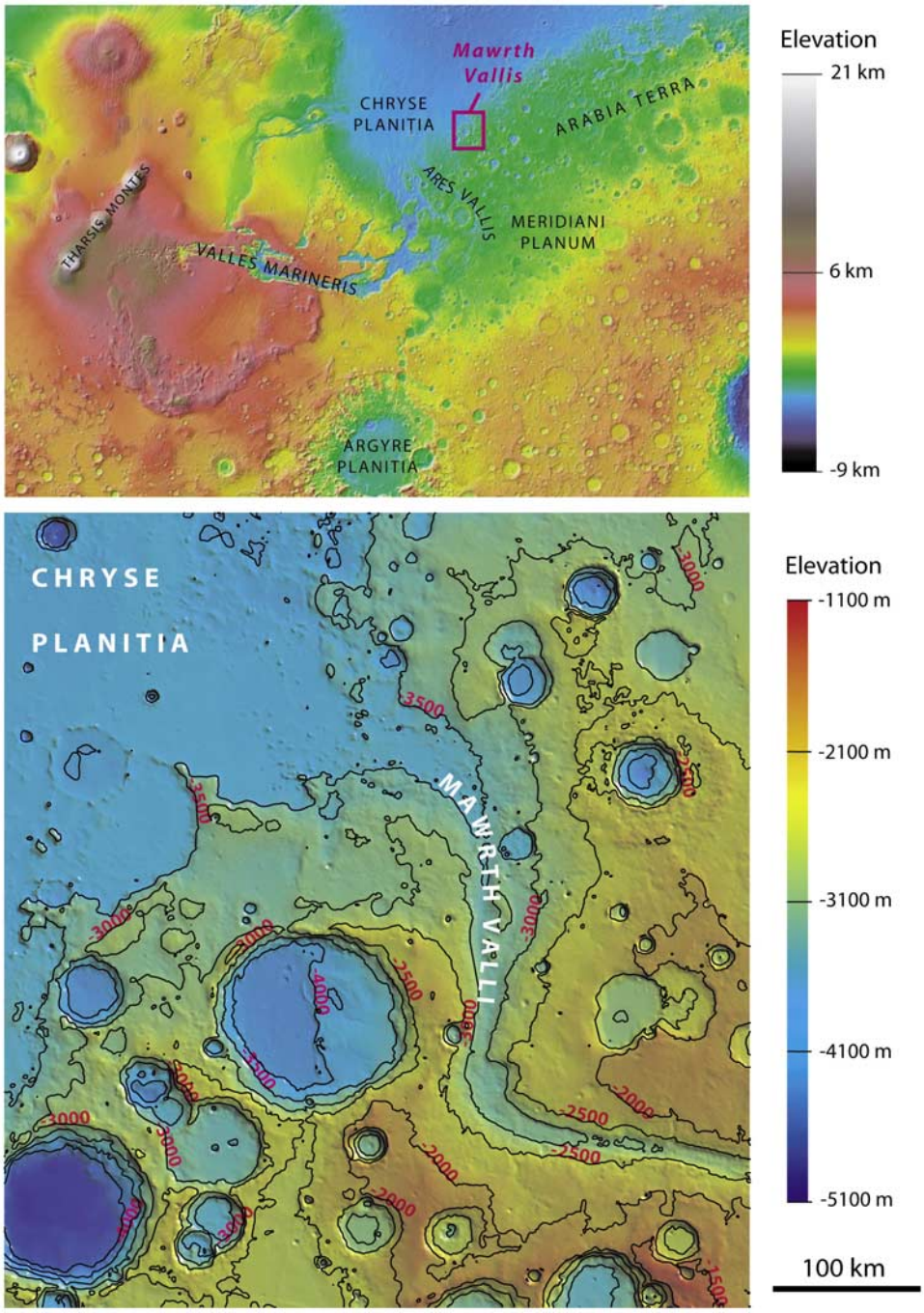

Figure 1. (top) Localization of the Mawrth Vallis region on the MOLA topography, on the limit of the Martian dichotomy. The box indicates the close-up of the second image. (bottom) MOLA topography of the Mawrth Vallis region. The border of Chryse Planitia is on the right of the image (altitude around −3800 m), and Mawrth Vallis cuts the Noachian highly cratered terrains in the large left part of the image.

OMEGA has detected, and the geological study of the phyllosilicate-rich zones.

2. Instruments and Data Sets

2.1. OMEGA Near-Infrared Data Set

[4] OMEGA is a visible and near-infrared (VNIR) hyperspectral imager providing three-dimensional data cubes with spatial samplings from a few kilometers to 300 m, and for each pixel the spectra between 0.35 and 5.1 μm, using 352 contiguous spectral elements (spectels), 7–20 nm wide. The spectrometer consists of three detectors (from 0.35 to 1 μm, from 0.9 to 2.7 μm, and from 2.5 to 5.1 μm) [*Bibring et al.*, 2004]. This study will use the data recorded by the second detector, which is well calibrated. This wavelength domain

is dominated by solar reflection and enables the identification of numerous minerals [*Bibring et al.*, 2005].

[5] Data processing first takes into account the modular transfer function of each spectel, the solar spectrum and the absorption due to the atmosphere (assuming a power law variation of CO_2 absorption with altitude). The output spectra equivalent to apparent I/F reflectance (flux received by the detector from the surface of Mars divided by the solar flux at Mars distance) can be used to retrieve the mineralogy of the surface of Mars by studying absorption bands. The analysis is based on the estimation of the band depth of characteristic bands in the 0.9−2.7 μm domain: we calculate the spectral index of these bands, which leads to the determination of the presence of some minerals or groups of minerals in the top tens of micrometers of the surface. One issue with the interpretation is the unavoidable mixing of minerals at the surface, as each spectrum corresponds to the large area of one pixel (at least 300 m × 300 m at the highest resolution), and several minerals must be present. However, some spectral features clearly show up and have already demonstrated the mineral diversity on the Martian surface [*Bibring et al.*, 2005].

[6] At the time of the submission of this paper, the region of Mawrth Vallis we studied has been covered by OMEGA at different spatial resolution during several orbits: three orbits at low resolution (around 3 km/pixel, 128 pixel large bands, orbits #353, #401 and #434); 3 orbits at medium resolution (less than 1.5 km/pixel, 64 pixel large band, orbits #2229, #2240 and #2262); and 19 orbits at high resolution (less than 1 km/pixel, 32 pixel large bands, orbits #912, #923, #934, #945, #967, #978, #989, #1000, #1011, #1293, #1326, #1337, #1348, #2960, #2971, #2982, #2993, #3004 and #3319).

2.2. THEMIS and TES Thermal Data Set

[7] The region of Mawrth Vallis has also been covered in the thermal infrared domain by the THEMIS camera. The THEMIS images displayed in this study show the retrieved temperature of the surface, with an uncertainty of ∼1 K [*Christensen et al.*, 2003], over each single orbit, both by day and night: mosaics of all available THEMIS temperature images in the Mawrth Vallis region at the time of the submission of this manuscript are displayed in Figure 2, for both daytime and nighttime data. The spatial sampling is around 100 m/pixel; the brighter the pixel, the warmer the surface. Over the whole mosaic, the temperature goes from ∼160 K to ∼207 K on the nighttime mosaic, and from ∼210 K to ∼270 K for the daytime mosaic. For a better mapping, the grey scale of some of these images has been adapted to the rest of the images. The interest of the THEMIS temperature of the surface at night is that it provides information about the thermal inertia of the surface, determined in this case by the physical properties of the top decimeter of the ground. In addition, the Mars Global Surveyor Thermal Emission Spectrometer (TES) [e.g., *Christensen et al.*, 2001] provides a global map of the Martian surface thermal inertia [*Putzig et al.*, 2005; *Mellon et al.*, 2000], but the 3 km pixel gives results at lower spatial resolution than THEMIS.

[8] The thermal inertia gives clues about some of its physical properties, like its induration, particle size, or density [*Pelkey et al.*, 2003; *Mellon et al.*, 2000; *Presley and Christensen*, 1997]. A high thermal inertia suggests either a highly indurated rock, a high density, or a large average particle size. A low thermal inertia indicates a poorly indurated fine grained material such as dust deposits. On Mars, the dustiest surfaces have TES thermal inertia smaller than 100 J m^{-2} K^{-1} $s^{-1/2}$, while the thermal inertia of the rockiest regions are higher than 550 J m^{-2} K^{-1} $s^{-1/2}$. In the Mawrth Vallis region, the thermal inertia varies from 200 to 500 J m^{-2} K^{-1} $s^{-1/2}$ [*Putzig et al.*, 2005]. The numerical values of the thermal inertia from THEMIS data are not retrieved in this study, but the comparison of the relative temperature of different surfaces can help to differentiate the geological units, and give clues about the physical properties of the material.

2.3. HRSC, MOC, and HiRISE Visible Data Sets

[9] HRSC (High Resolution Stereo Camera) is a pushbroom high resolution camera on board the ESA/Mars Express mission. It has been designed to get wide images with an up to 10 m/pixel spatial sampling, with color and stereo channels [*Neukum and Jaumann*, 2004]. Only the data provided by the nadir line detector have been used in this study, for orbits #1293, #1326, #1337, with a resolution around 14 m/pixel. The HRSC mosaic (Figure 3) compiles these data, covering the whole region that has been studied with OMEGA. This camera is the only one to offer a total coverage of this region at such a high resolution in the visible domain. The HRSC mosaic (Figure 3) is accompanied by a simplified geomorphologic map of the region showing the main units and landforms.

[10] In addition, we used MOC narrow angle images. This camera offers high spatial resolution imagery, with spatial sampling from 2 to 6 m/pixel, but no full coverage. At the time of the submission of this paper, HiRISE (the High Resolution Imaging Science Experiment of the Mars Reconnaissance Orbiter mission) [e.g., *McEwen et al.*, 2007] has delivered one image obtained in the region of Mawrth Vallis (TRA_000847_2055). This instrument can offer images with spatial resolution of less than 30 cm/pixel.

3. Geologic and Mineralogical Properties

3.1. Geologic Context

[11] The studied area is composed of two main units: Chryse Planitia and the Noachian plateaus. Chryse Planitia is the large dark unit (TES albedo around 0.11) extending toward the northwest in Figure 3, upon which several wind streaks indicate the main wind direction, from northeast to southwest. Chryse planitia is a large depression (up to 1800 km across) in which several outflow channels debouche; near the Mawrth Vallis mouth, it lies between −3700 and −3900 m (all altitudes are given with respect to the MOLA areoid) in altitude (Figure 1), and has higher temperature than the rest of the region on THEMIS nighttime data (Figure 2). The Noachian plateaus are principally divided into bright outcrops and dark material on visible data set (Figure 3). They stand above −3300 m in altitude, and generally more than 1000 m above Chryse Planitia. THEMIS show large differences in temperature between the units in both the nighttime and daytime data, revealing differences in the induration, grain size, or rock exposure of the surfaces, which are discussed in section 3.2.

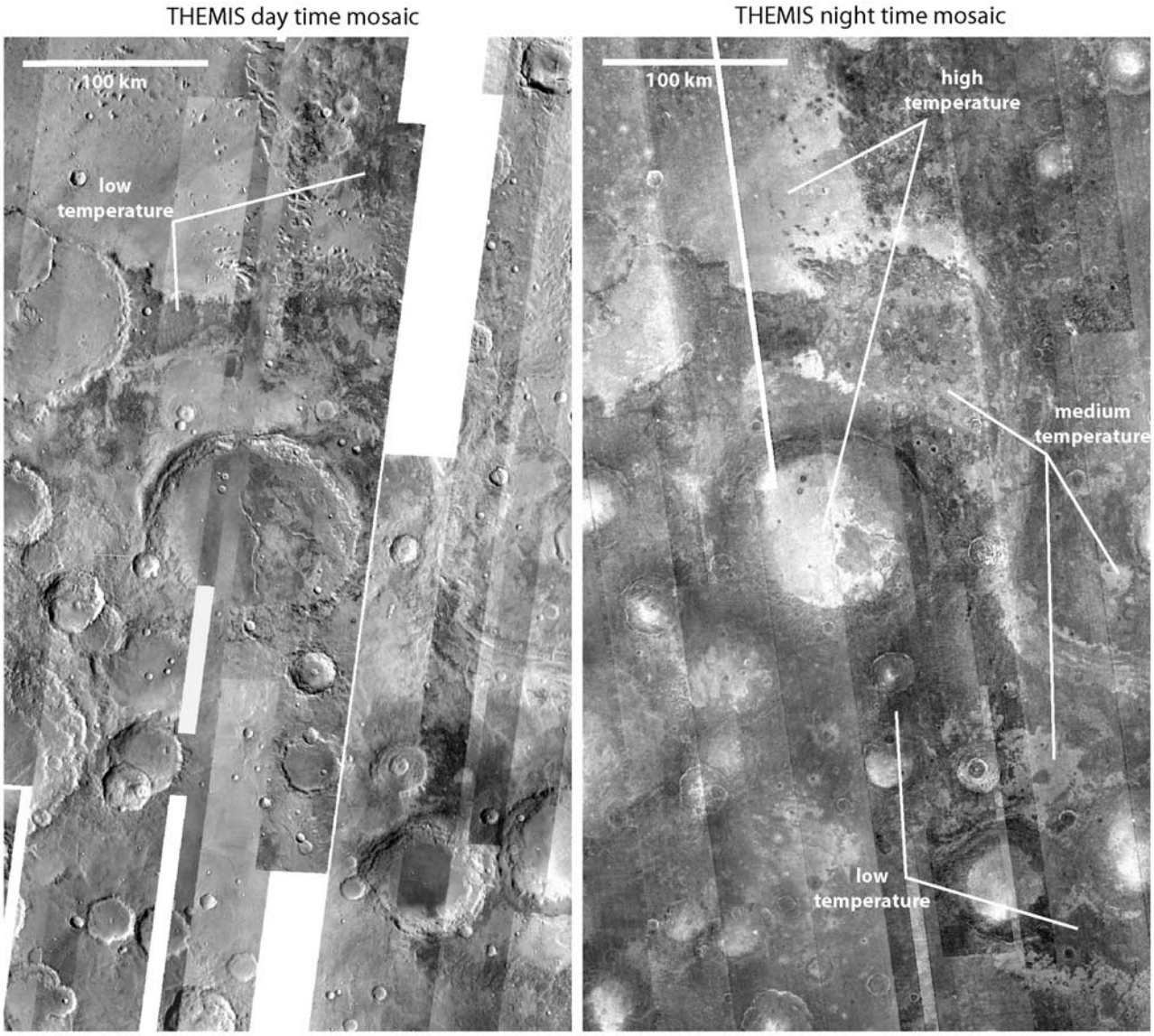

Figure 2. Mosaics of THEMIS thermal images of the Mawrth Vallis region. Bright tone shows warmer temperature, and dark tone shows colder temperature. (left) Mosaic of THEMIS daytime temperature images (resolution: 100 m/pixel; temperature goes from ~210 K to ~270 K, although, as the temperature range changes from one orbit to another, we did not compose a scale bar for the whole mosaic). (right) Mosaic of THEMIS nighttime temperature images. The grey scale has been adapted for a few orbits to fit to the mosaic (resolution: 100 m/pixel; temperature goes from ~160 K to ~207 K; for the same reasons as the daytime mosaic, we did not compose a scale bar for the whole mosaic); the warmest surfaces are located mainly on the floor of Chryse Planitia, on the mouth of Mawrth Vallis, and on the crater floors.

[12] The main fluvial landform consists of the Mawrth Vallis outflow channel. Mawrth Vallis crosscuts the Noachian plateaus, and is dated approximately to the Early Hesperian or Late Noachian epoch [*Scott and Tanaka*, 1986]. Mawrth Vallis debouches onto the floor of Chryse Planitia at an altitude around −3800 m (Figure 1). The floor of Mawrth Vallis has a relatively higher temperature on nighttime THEMIS imagery, particularly at its mouth (Figure 2). The channel flowed from south to north as deduced from a few streamlined islands and the topography. In addition, a few valleys are present on the Noachian plateaus, with some of them cutting Mawrth Vallis flanks. Small valleys also exist on the floor of crater A at the center of the mosaic (Figure 3).

[13] Only few structural patterns are present in the region. There is a major fault in the middle of crater A that creates a topographic step, up to 200 m in elevation (Figure 3). This fault appears as a compressive fault on HRSC and THEMIS data sets similar to those mapped by *Watters* [1993] in the cratered highlands. It continues to the north, where it crosses a part of the Noachian plateaus but not Chryse Planitia, implying an older age than Chryse Planitia.

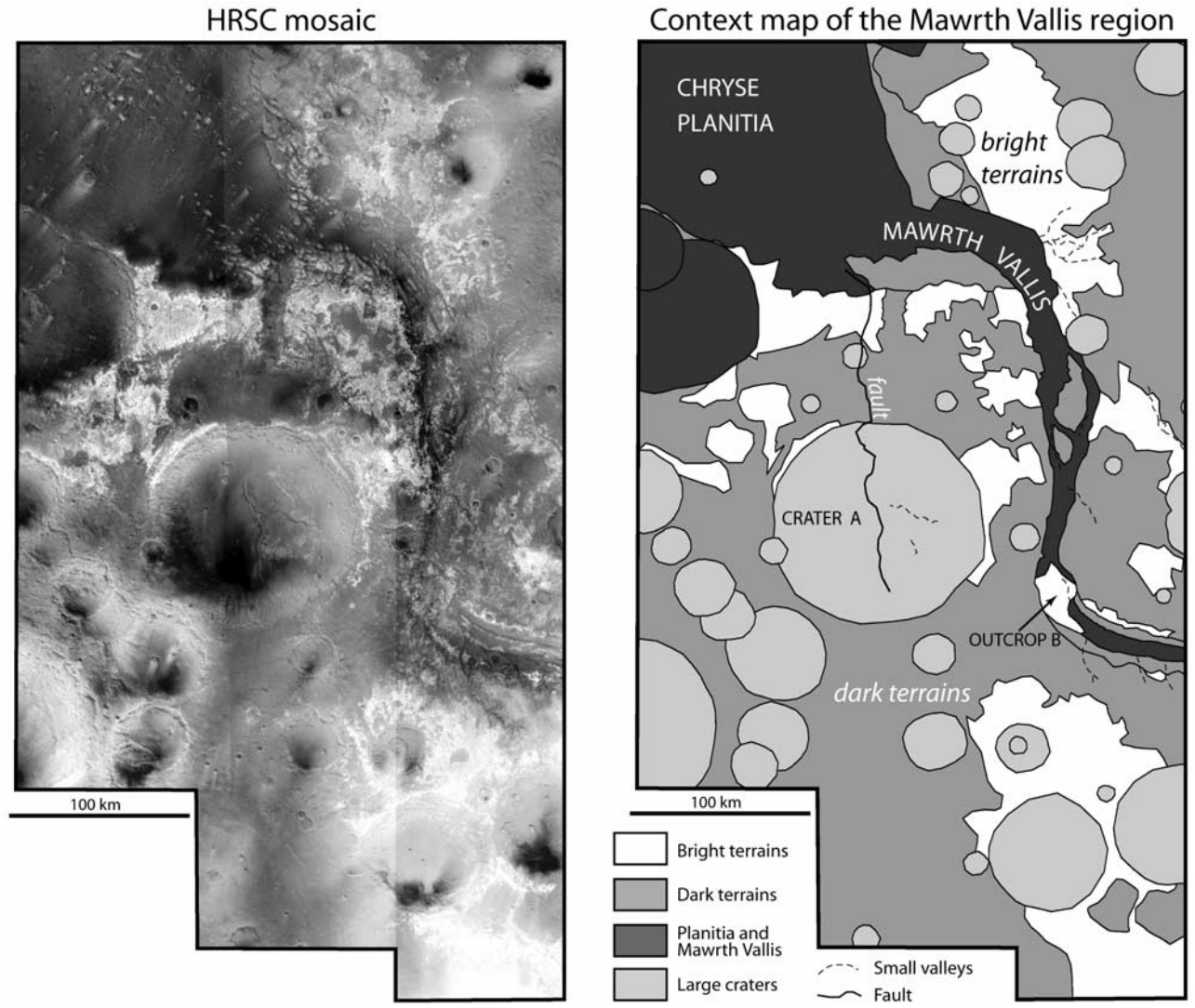

Figure 3. (left) Mosaic of three HRSC nadir images (resolution: ~14 m/pixel) covering the Mawrth Vallis region. (right) Context map of the Mawrth Vallis region with indication of the principal features.

3.2. Regional Mineralogical Units

[14] OMEGA identified two classes of minerals in the Mawrth Vallis region: pyroxenes and phyllosilicates. We present here the parallel investigation of the mineralogy and geomorphology of these two classes of minerals.

3.2.1. Mafic Minerals

3.2.1.1. Spectral Signature

[15] Some OMEGA spectra show two broad bands centered around 1.0 μm and 2.2 μm revealing the presence of pyroxenes. The positions of the centers of these bands vary with the calcium content in the pyroxene. For a high calcium pyroxene (HCP), the centers are around 1.05 and 2.30 μm, and for a low calcium pyroxene (LCP), around 0.9 and 1.8 μm. Both types of pyroxenes have been identified on Mars by OMEGA [*Mustard et al.*, 2005] and recently confirmed by TES [*Rogers and Christensen*, 2007]. In Figure 4a an OMEGA spectral ratio displays pyroxene absorption features, compared to laboratory clinopyroxene spectra (HCP, here Augite NMNH120049, USGS spectral library [*Clark et al.*, 1993], specific minerals discussed in this study are referenced in Table 1). The broad bands are centered around 1.0 and 2.2 μm, indicating principally HCP, but the bands are large and so the surface is very likely a mix of HCP with some LCP. The reflectance of the corresponding pixels, taken at 1.08 μm on OMEGA, is in the range of 0.08 to 0.13. Concerning olivine, OMEGA cannot detect its presence when the olivine represents less than 20% of the surface material (depending of the size of the grains) [*Poulet et al.*, 2007]: in the Mawrth Vallis region, OMEGA spectra do not show any olivine detection, but this does not exclude totally the presence of olivine, if present in small amount.

[16] Pyroxene-rich areas are mapped using the calculation of a spectral index of the very broad ~2.2 μm band that occurs in the spectra of the Mawrth Vallis region. This spectral index is calculated as expressed in Table 2.

3.2.1.2. Corresponding Terrains and Physical Properties

[17] When superimposed on HRSC visible images (Figure 5, left), pyroxene is found only in low albedo areas. Nevertheless, three different types of pyroxene-rich areas can be

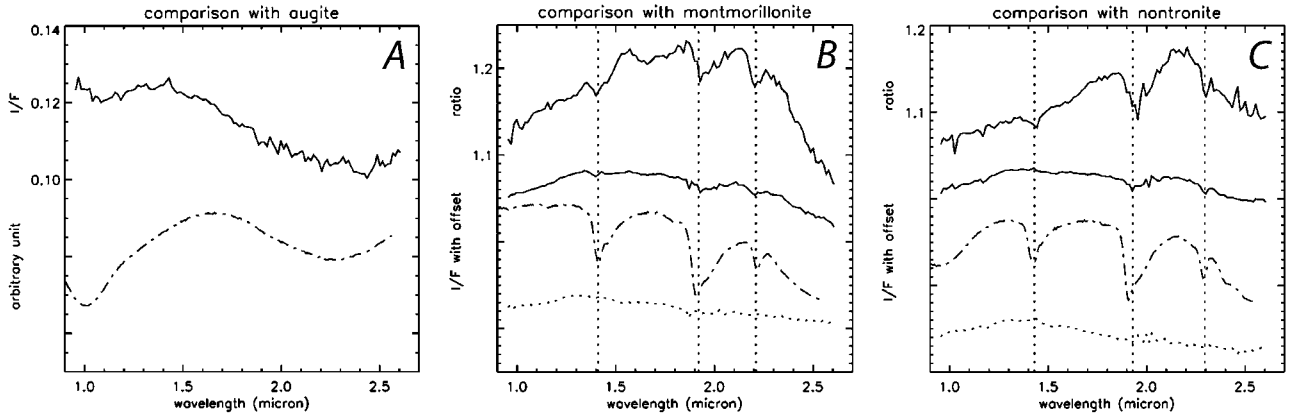

Figure 4. (a) Average of six OMEGA spectra (solid line) with pyroxene detection, compared with a laboratory spectrum of augite (clinopyroxene, dashed line, from USGS spectral library). (b and c) Smectite spectra as identified by OMEGA in the Mawrth Vallis region. (b) From bottom to top: the dotted line is the OMEGA reference spectrum; the dot-dashed line is a laboratory spectrum of montmorillonite (USGS spectral library); the bottom solid line is the average of 6 OMEGA spectra, and the top solid line is the ratio of this average over the reference spectrum. (c) The same for other pixels compared with nontronite (Fe-smectite, USGS spectral library).

seen on HRSC and THEMIS: (1) crater floors, where the pyroxene signature is stronger on the southwest flanks of large craters (>10 km); (2) in Mawrth Vallis mouth and Chryse Planitia; and (3) on the darkest surfaces of the Noachian plateaus. In cases 1 and 2 (i.e., the biggest craters, Chryse Planitia and Mawrth Vallis mouth), the apparent nighttime temperature is the highest of the region (i.e., very bright on the nighttime image). This comes from the high thermal inertia of these surfaces, suggesting mainly rocky areas, high induration or very coarse grained surface, which is indeed consistent with the TES thermal inertia in the range of 400 to 500 J m^{-2} K^{-1} $s^{-1/2}$ [*Putzig et al.*, 2005]. In case 3, on the plateaus, the pyroxene-rich areas are the coolest surfaces of the region by nighttime: cooler than in cases 1 and 2, and also cooler than the rest of the plateaus, suggesting finer grained material. This is confirmed by the relatively low TES thermal inertia of those terrains, around 250 J m^{-2} K^{-1} $s^{-1/2}$ [*Putzig et al.*, 2005].

[18] The mineralogy of Chryse Planitia and its high thermal inertia support the proposal that its surface was formed by lava flows [*Scott and Tanaka*, 1986]. The low albedo areas on the southwest side of the large crater floors have been interpreted as aeolian sand deposits [*Edgett*, 2002]. The presence of pyroxene correlated to this low albedo and medium thermal inertia region, and the correspondence of the SW side with the main wind directions, confirm this interpretation as volcanic coarse grained sand accumulated by the winds. Coarse sand, with a large average particle size (>900 μm), can effectively lead to a thermal inertia of 400 J m^{-2} K^{-1} $s^{-1/2}$ or higher [*Pelkey et al.*, 2001, 2003; *Presley and Christensen*, 1997]. On the Noachian plateaus, the low thermal inertia could be due to the presence of a poorly indurated pyroxene-rich material, constituted of finer grains than in the other low albedo terrains of the region. This dark material actually drapes over the Noachian plateaus almost uniformly, which would indicate an airfall deposition after transport of suspended fine particles in the atmosphere [*Edgett*, 2002]. A geomorphic and spectroscopic analysis (with ISM, Imaging Spectrometer, on board Phobos 2) of a similar dark mantle in west Syrtis Major suggested an airfall deposition of dust mixed with sand, with a large proportion of iron oxides and/or pyroxenes, about 50–60% [*Poulet et al.*, 2003].

3.2.2. Hydrous Phyllosilicates

3.2.2.1. Spectral Signatures

[19] A narrow absorption band centered at 1.93 μm appears in spectra of several surfaces of the region. This band is due to the combination of the H-O-H bend, ν_2 at ~6.1 μm, and a symmetric OH stretch, ν_3 at ~2.9 μm [*Clark et al.*, 1990], and reveals the presence of hydrous minerals like sulfates, hydroxides or phyllosilicates. There is also, for the spectra of the same pixels, a characteristic band at 1.41 μm, due to the combination of OH vibration modes. Due to the weakness of the band, it generally appears only in spectral ratios. These two bands at 1.93 and 1.41 μm are not specific to hydrous phyllosilicates, but,

Table 1. Names, Chemical Formulae, and Absorption Bands of the Minerals Discussed in This Study[a]

Candidate Minerals Discussed	Example From the USGS Spectral Library	Chemical Formula	Positions of the Detected Absorption Bands
HCP (clinopyroxenes)	Augite NMNH120049	$(Ca,Mg,Fe)_2(Si,Al)_2O_6$	1.0 μm, 2.2 μm
Al-OH smectites	Montmorillonite SCa-2.a	$(Na,Ca)_{0.3}(Al,Mg)_2Si_4O_{10}(OH)_2{\cdot}nH_2O$	1.4 μm, 1.93 μm, 2.20 μm
Fe-OH or Mg-OH smectites	Nontronite NG-1.a (Fe-OH smectite)	$Na_{0.3}Fe^{3+}{}_2(Si,Al)_4O_{10}(OH)_2{\cdot}nH_2O$	1.4 μm, 1.93 μm, 2.30 μm

[a]Concerning the smectites, montmorillonite and nontronite are examples, and the presence of other smectites is possible.

Table 2. Description of Spectral Indices Used in This Study[a]

Candidate Minerals	Characteristic Absorption Band Center	Spectral Index	Detection Threshold
HCP (clinopyroxene)	2.2 μm	1 − (R(2.15) + R(2.20))/(R(1.81) + R(2.50))	1%
Hydrous minerals	1.93 μm	1 − (R(1.93) + R(1.94))/(R(1.80) + R(2.12))	2%
Al-OH smectites	2.20 μm (along with 1.93 μm)	1 − (R(2.19) + R(2.20))/(R(2.15) + R(2.27))	2%
Fe-OH or Mg-OH smectites	2.30 μm (along with 1.93 μm)	1 − R(2.30)/(0.25*R(2.26) + 0.25*R(2.27) + 0.5*R(2.34))	2%

[a]R is the reflectance I/F at the given wavelength in μm.

for most of the pixels showing those bands, other narrow bands are seen by OMEGA, centered on 2.20 and 2.30 μm. For phyllosilicates, bands occurring between 2.0 and 2.5 μm are generally caused by the combination of OH stretch and metal-OH bend. At 2.20 μm, absorption is mainly due to the Al-OH bond, whereas around 2.30 μm, the band can either be due to Fe-OH (at 2.29 μm) or Mg-OH (>2.32 μm), or a mixing of the two [*Clark et al.*, 1990; *Poulet et al.*, 2005].

[20] Figures 4b and 4c show OMEGA spectral ratios compared to laboratory spectra of nontronite and montmorillonites; the ratio over dusty terrain spectra enhances the 1.41, 1.93 and 2.20 or 2.30 μm bands. Those comparisons with terrestrial minerals (Nontronite NG-1.a and Montmo-

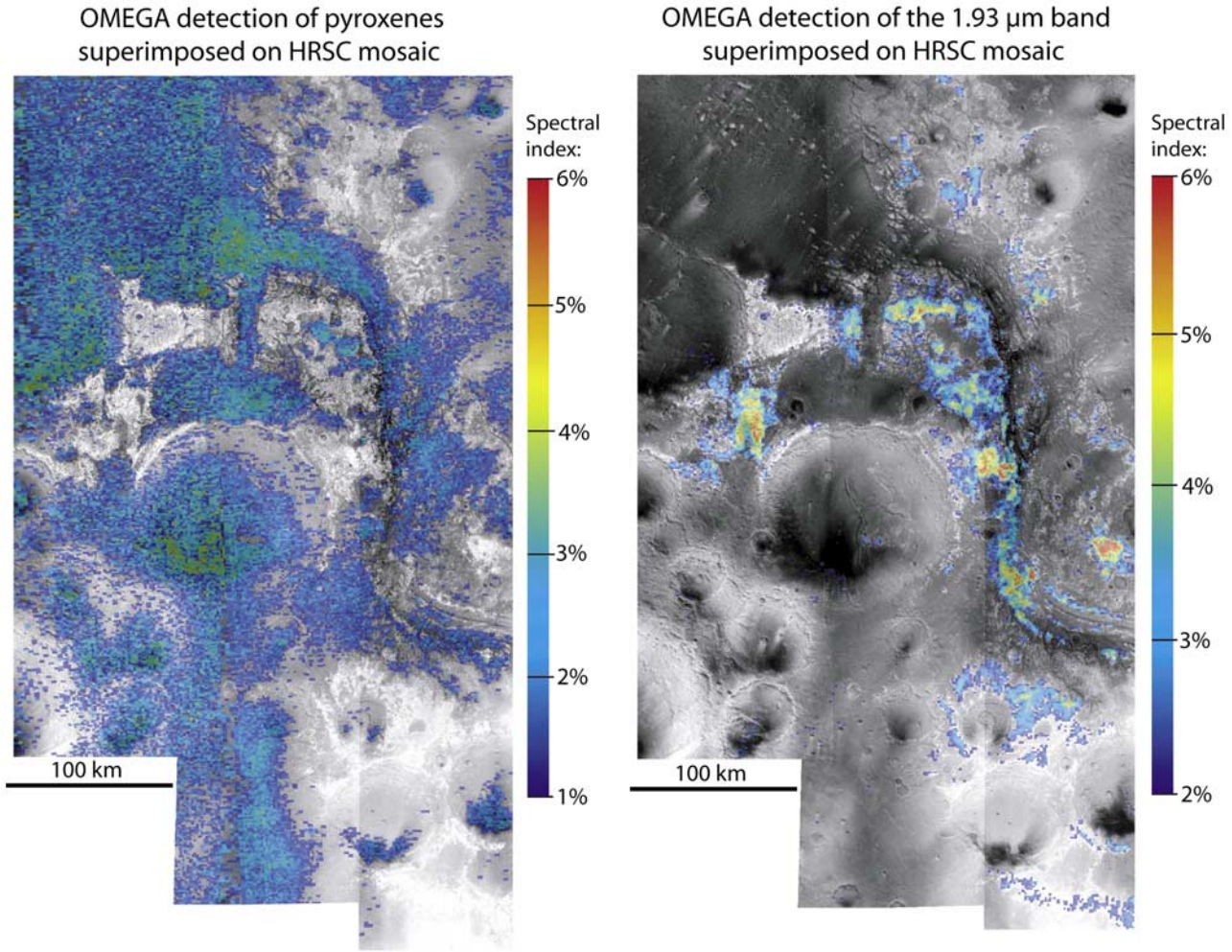

Figure 5. (left) HRSC nadir images mosaic superimposed with the spectral index of the pyroxene 2.2 μm band as derived from OMEGA data. This band characterizes the detection of pyroxenes. These pyroxenes are located on dark terrains, either on the floor of Chryse Planitia, Mawrth Vallis, and the craters or on the plateaus in some zones. (right) HRSC nadir images mosaic superimposed with the spectral index of the 1.93 μm band as derived from OMEGA data. This band characterizes the detection of hydrated minerals. These hydrated minerals are located here exclusively on bright outcrops, and mainly on the plateaus. A more precise classification of these hydrated minerals was conducted afterward thanks to the detection of the 2.20 and 2.30 μm bands on the same surfaces and is displayed in Figure 6.

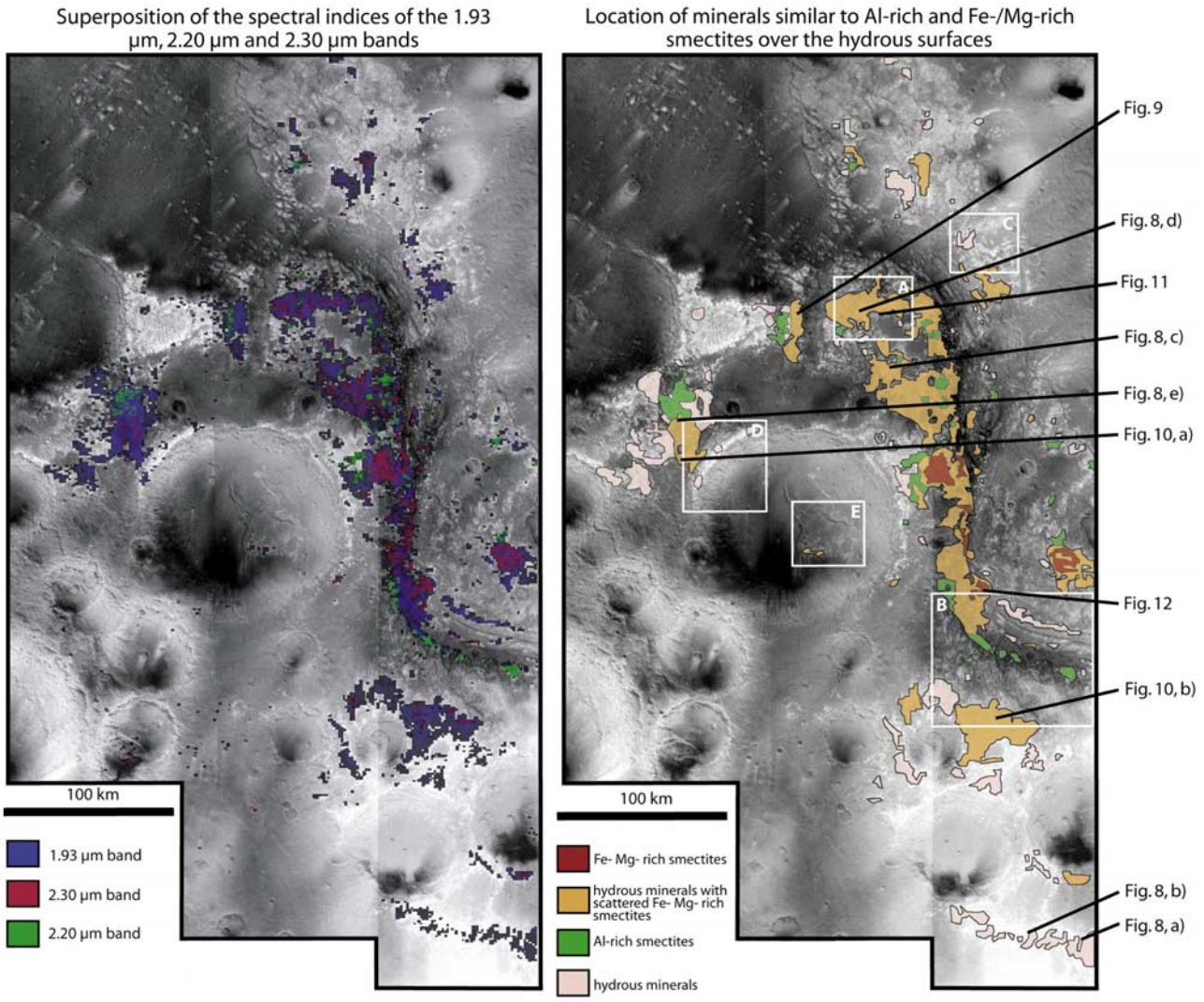

Figure 6. (left) HRSC nadir image mosaic superimposed with the spectral index of the 1.93 μm, 2.20 μm, and 2.30 μm bands. (right) Supposed nature of the minerals detected with OMEGA. In red are Mg-OH and/or Fe-OH smectites comparable to nontronite and in green are Al-OH smectites comparable to montmorillonites, whereas the orange surface delimits areas where Fe- and Mg-rich smectites are seen only on a few scattered pixels. In light pink are surfaces where the discrimination is not straightforward, due to the weakness of the bands. The white boxes delimit the close-ups displayed in the following figures: white box A, Figure 7; white box B, Figure 13; white box C, Figure 14; and white boxes D and E, Figures 15a and 15b. The black lines point to the locations of the MOC images of Figures 8, 9, 10, and 12 and HiRISE images of Figure 11.

rillonite SCa-2.a, USGS spectral library [*Clark et al.*, 1993]; see Table 1) indicate that those bands are due to the presence of smectites, a group of phyllosilicates. The corresponding OMEGA surface spectra are similar to the spectrum of Fe-rich smectites, with a 2.30 μm band, such as for nontronite (Fe-rich smectite) or to Al-rich smectites, involving a band at 2.20 μm such as for montmorillonites. Mg-rich smectites such as hectorite or saponite are possible alternative end-members with a 2.3 μm band, but Mg-OH bonds are usually shifted to values in the range of 2.30–2.34 μm whereas Fe-OH is found at 2.29 μm. A mixture of Fe- and Mg-smectites is also not excluded. From now on, we will speak about "phyllosilicate-rich zones" to refer to the overall areas which display spectra similar to those smectites. These zones have reflectance at 1.08 μm ranging from 0.19 to 0.30 in OMEGA data.

[21] Finally, it is also important to note that amorphous silica, quartz or plagioclase have no significant signatures or very weak signatures in the near infrared, so the presence of such minerals in the bright terrains is not excluded.

3.2.2.2. Mapping and Corresponding Terrains

[22] The mapping of hydrous minerals has been made with the spectral index of the 1.93 μm band, as this band is the strongest band observed in the 0.9 to 2.6 μm domain for hydrous minerals, and is present in every phyllosilicate mineral spectrum provided by OMEGA. Figure 5, right, shows a full mapping of the outcrops rich in hydrous minerals of the Mawrth Vallis region, characterized by the

spectral index of the 1.93 μm absorption band (see Table 2 for the calculation of the spectral index), superimposed on the HRSC mosaic.

[23] The same areas reveal 2.30 or 2.20 μm absorption bands, differentiating the Fe-OH smectites and Al-OH smectites on most of the surfaces mapped with the 1.93 μm band (Figure 6). The spectral indices for these two absorption bands are calculated as expressed in Table 2. A threshold of 2% is used in order to take into account the instrumental noise [*Poulet et al.*, 2007]. Figure 6 illustrates the locations of these smectites in the Mawrth Vallis region, showing in green the Al-OH smectites, in red the Fe-OH or Mg-OH smectites, and in orange the surfaces where several pixels only show Fe- or Mg-smectites. This last category likely correspond to outcrops where the absorption bands of some pixels is too weak to show any 2.30 or 2.20 μm band but only the 1.93 μm band. This map shows that the Fe-OH smectites are predominant in the Mawrth Vallis region.

[24] In the area indicated in pink, the band depths are not deep enough to determine the type of the hydrous minerals; therefore many hydrous minerals could be invoked. However, these areas do not reveal any other spectral features such as those indicating sulfates. Furthermore, these areas have weak 1.93 μm absorption band, with spectral index close to 2%. As the 1.41, 2.20–2.30 μm bands are weaker than the 1.93 μm band for all library spectra of phyllosilicates, surfaces where the latter is weak could show only this band despite being phyllosilicate-rich. Thus areas indicated in pink contain hydrous minerals, which would likely correspond to phyllosilicates.

[25] As seen in HRSC imagery, phyllosilicate-rich terrains are located on top of the Noachian plateaus, at altitudes from −3200 m to −2200 m, correlated with medium to high albedo terrains (reflectance from 0.19 to 0.30 at 1.08 μm in OMEGA data). OMEGA detects phyllosilicates on surfaces between the great impact craters but not on large crater floors. The outcrop on the floor of crater A (Figure 3) where the albedo is higher is an exception. One particular place on the floor of Mawrth Vallis, where a phyllosilicate signature is also displayed, occurs at −3300 m, at about 23.0°N, 18.2°W, at a bend of the channel, named outcrop B on the context map in Figure 3. These last two particular locations will be discussed in points 4.2 and 4.3.

[26] On THEMIS nighttime IR images, the phyllosilicate-rich areas correspond to relatively warm terrains on the Noachian plateaus compared to the surrounding pyroxene-rich dark material. The TES thermal inertia map indicates a thermal inertia around 300 to 400 J m^{-2} K^{-1} s$^{-1/2}$ for those outcrops [*Putzig et al.*, 2005]. This can be explained by a higher degree of induration or coarser grains for the phyllosilicate-rich terrains than the surrounding dark material. Using HRSC, THEMIS and TES, the characteristics of the phyllosilicate-rich areas can be summarized as (1) bright terrain on HRSC imagery, with corresponding reflectance from 0.19 to 0.30 at 1.08 μm in OMEGA data, and (2) medium nighttime temperatures on THEMIS data and intermediate TES thermal inertia of 300–350 J m^{-2} K^{-1} s$^{-1/2}$.

[27] The close-up in Figure 7, visible and infrared images of the same outcrop, illustrates these observations (see Figure 5 for the location). The dark material in the HRSC visible image (Figure 7a) corresponds to a pyroxene-rich material (Figure 7d), warm by day (Figure 7b) and relatively cold by night (Figure 7c), induced by a low thermal inertia. This dark material seems to be superimposed on the bright material on daytime THEMIS temperatures (Figure 7b). In contrast, the detection of the 1.93 μm band (Figure 7e) points toward high albedo terrains on visible image (Figure 7a). The 2.30 μm band (Figure 7f) is clearly correlated to the 1.93 μm band indicating here Fe-OH smectites. The lower temperature by day (Figure 7b) and higher temperature by night (Figure 7c) reveal a higher thermal inertia of this outcrop than the surrounding dark material. The daytime image shows morphologic features in the phyllosilicate area; it is dissected with residual buttes indicating strong erosion. Notice that the area between phyllosilicates and pyroxene-rich surfaces in Figure 7c does not show any particular signature within the limits of detection (minimum of 2% for the spectral index). This surface seems less eroded on the daytime THEMIS image, possibly explaining this area as a transition zone without a clear signature on OMEGA spectra, as for a mixture of different materials.

4. Detailed Geomorphology of the Phyllosilicate-Rich Outcrops

4.1. Surface Characteristics at MOC and HiRISE Scale

[28] The HRSC mosaic shows the strong correlation of phyllosilicates with bright terrains. When observed on MOC narrow angle images at a resolution better than 5 m/pixel, the phyllosilicate-rich zones exhibit widespread layering (Figure 8). These layers are clearly associated with the bright surface when eroded along local slopes (Figures 8a, 8b, and 8e and Figure 9). On flatter areas, terrains are etched by erosion where residual buttes are present and layers are more difficult to see but are present locally (Figures 8c and 8d). Layering is also visible on the scarp of ~1 km diameter craters (Figure 10). In all images, the layers are generally very thin, apparently a few meters thick. These layers correspond to a part of the light toned layered deposits extensively mapped in this region and all over the planet by *Malin and Edgett* [2000].

[29] A residual darker surface is present in some areas of these images. This surface is similar to the pyroxene-rich surface mapped in Figure 7d. At MOC scale, it confirms the interpretation of the pyroxene-rich areas as a thin mantle partly covering the region, as seen by residual small dark buttes left of Figure 8c. A few small craters are also filled by remaining dark material, when the mantle has been completely eroded from around those craters (Figures 8c and 8d). In Figure 8e, bright residual buttes are surrounded by a darker layer. Some of them could possibly correspond to inverted craters: a few impact craters were filled by layered material locally showing topographic inversion. The bright buttes and crater fills are layered in contrast to the surrounding darker surface. Furthermore, no MOC image showed any evidence of darker interbeds in the layered terrains.

[30] HiRISE shows the same characteristics at 29 cm/pixel: Figure 11 shows a small layered butte (right) and a 300 m large outcrop (left), displaying layers when well-exhumed at the bottom right of the image. In the last case, the dark mantling is thin, allowing us to see the heavily cratered surface at the top of the bright unit. This confirms

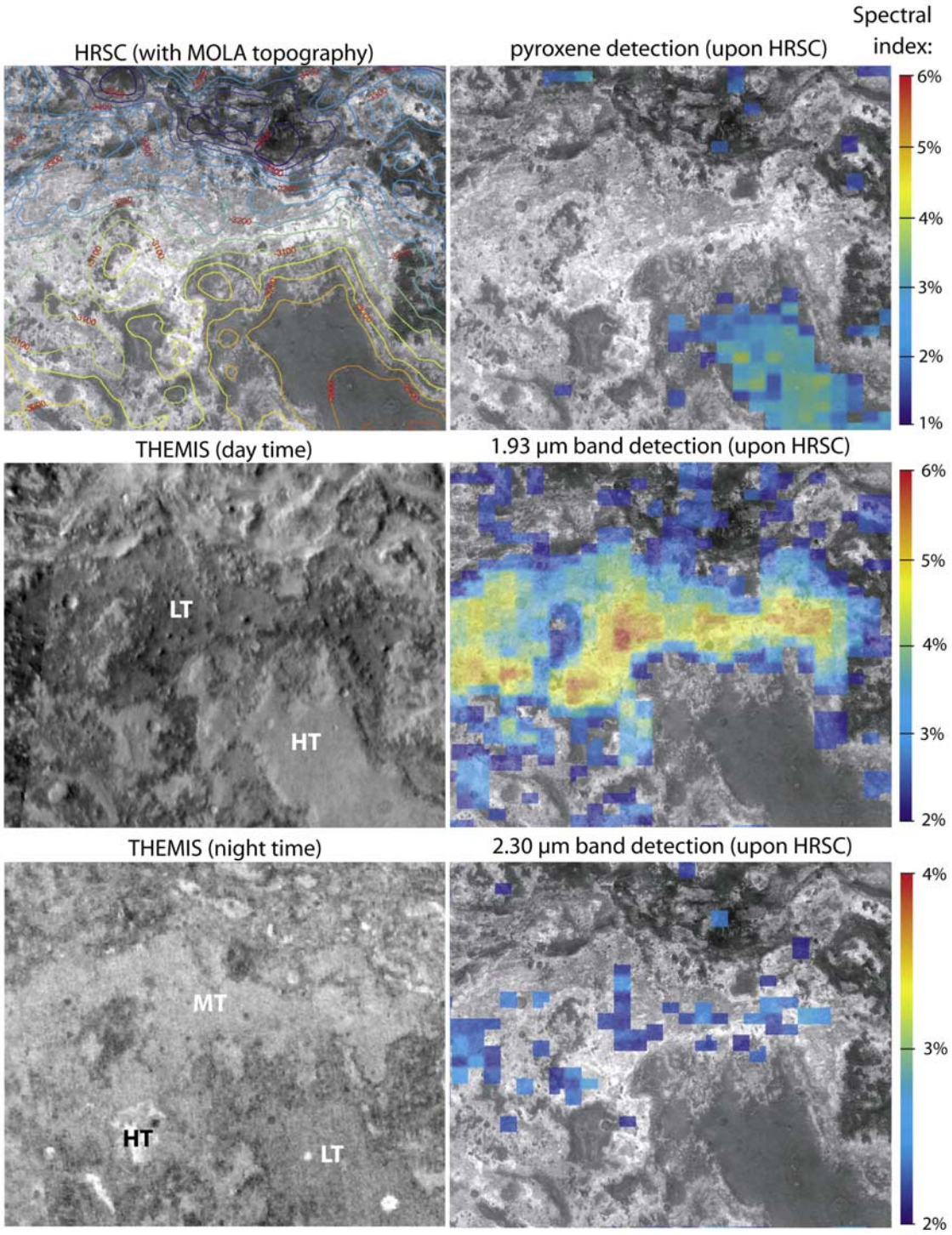

Figure 7. Close-up on the Noachian plateaus near Mawrth Vallis mouth (see Figure 6 for location and scale). From top to bottom and left to right: HRSC nadir image with MOLA topography; THEMIS daytime image (sunlight comes from the left); THEMIS nighttime image; pyroxene detection (spectral index of the band centered around 2.2 μm $\geq$ 2%) superimposed on the HRSC mosaic; hydrous mineral detection (spectral index of the 1.93 band $\geq$ 2%); and spectral index of the 2.30 μm band $\geq$ 2%. LT stands for low temperature, HT stands for high temperature, and MT stands for medium temperature.

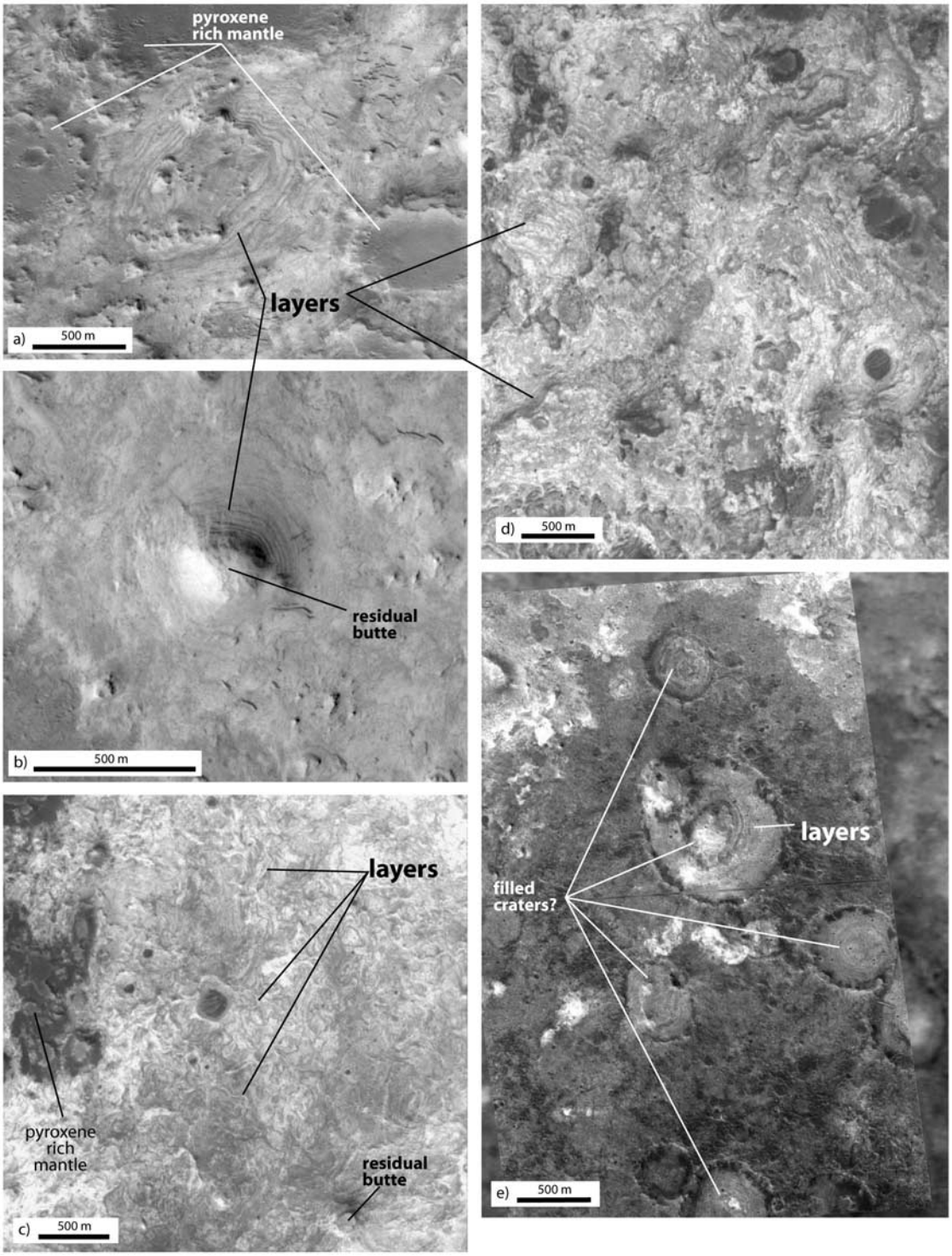

Figure 8. Images provided by the Mars Orbiter Camera in the Mawrth Vallis region. North is toward the top; sunlight comes from southwest. See Figure 6 for location. (a) R09_01962; (b) R05_01499; (c) E10_03929; (d) E14_00606; (e) S08_00601 superimposed on HRSC. All these close-ups correspond to terrains where spectra indicate Fe-OH smectites, but the Al-OH outcrops do not show any evident morphological difference.

the ancient age of this unit as seen from the crater saturation. Locations with few small craters are likely exhumed from beneath this heavily cratered surface. This process of exhumation could erase the small craters (<100 m), explaining why currently we see surfaces of the old phyllosilicate-rich crust with apparent younger crater retention ages.

[31] Hence there is in the Mawrth Vallis region a bright unit displaying meter-scale layers, rich in phyllosilicate

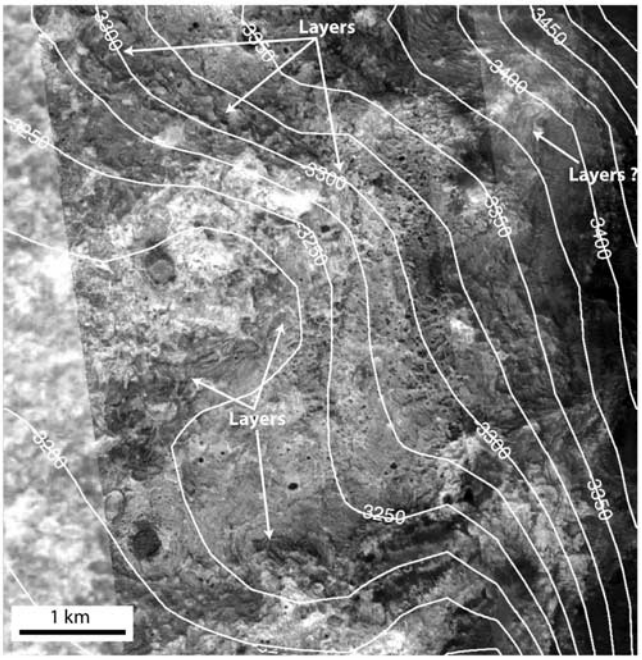

Figure 9. MOC mosaic of a phyllosilicate-rich outcrop west of Mawrth Vallis Mouth (see Figure 6 for location), with MOLA topography contours. The layers seen at different altitudes indicate a unit at least 150 m thick. The mosaic is superimposed on HRSC imagery, as visible on the left of the image.

minerals, and still partly covered by a pyroxene-rich dark thin mantle of various thicknesses, up to ~10 m.

[32] Figure 12 reveals the presence of fractures forming polygonal structures on phyllosilicate-rich terrains, on outcrop B (see context, Figure 3) on Mawrth Vallis floor. These polygons are from 100 to 800 m wide. As can be seen in Figure 12, these polygons affect only the bright outcrops, and not the dark mantle, so it seems that their formation predated the mantle deposition or was limited to the top of the bright outcrops. The geometry of these polygons is different from tectonic processes but fits the typical geometry of fracture networks produced by volume change, i.e., random orthogonal geometry [e.g., *Mangold*, 2005] with polygons of similar sizes. Those polygons might have formed by volume decrease due to changes of temperature in ice-rich subsurface (thermal cracks) or desiccation (mud cracks), possibly related to the end of the outflow channel activity. Smaller polygons (less than 10 m in width) appear on the HiRISE image (Figure 11, right) outside Mawrth Vallis floor, on the top of the Noachian plateaus (see Figure 6, right). Compared to the random orthogonal geometry (see *Mangold* [2005] for different types of geometry) of the polygons in Mawrth Vallis floor (Figure 12), the geometry of the fracture network is much more dense and heterogeneous in geometry and size without clear patterns. This geometry might not involve the same processes: for example, thermoclastism from diurnal cycles might be able to create cracks without ice or liquid water in the pore space. Nevertheless, the presence of clay minerals in that material might help this fracturing process because the interlayer water of clays contribute to create volume changes with variation of temperature or humidity [e.g., *Velde*, 1995].

4.2. Lack of Phyllosilicates on a Few Bright Outcrops

[33] The correlation of phyllosilicates with bright outcrops raises a question about the presence of bright outcrops devoid of phyllosilicates. For example, a large bright outcrop on the west of Mawrth Vallis mouth shows almost no evidence of the presence of phyllosilicates (see Figure 5), except a weak absorption at 1.93 μm around a crater 5 km in width, on the flank facing Chryse Planitia. In fact, when the bright areas on HRSC visible images do not correspond to phyllosilicate-rich surfaces, THEMIS IR nighttime

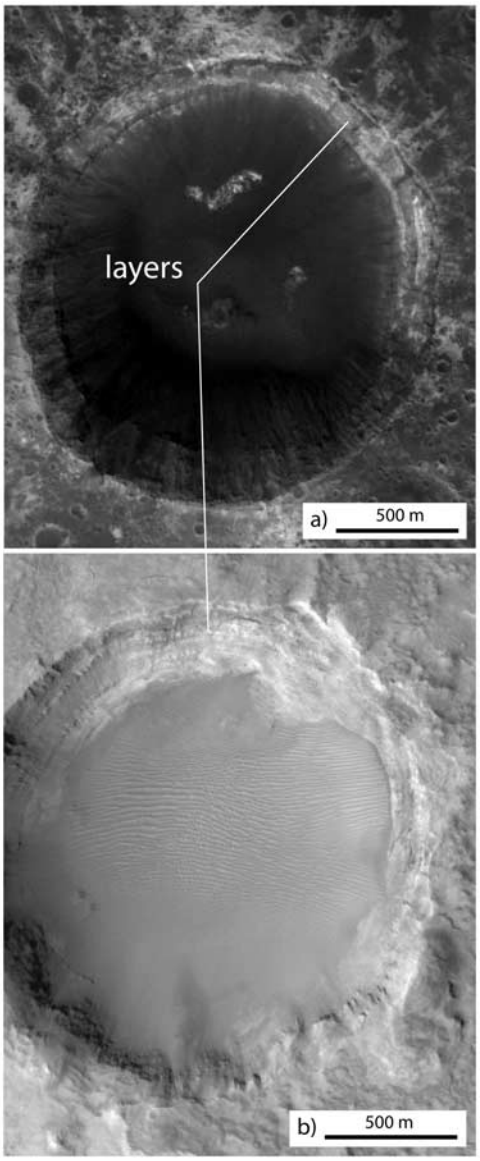

Figure 10. Images provided by the Mars Orbiter Camera in the Mawrth Vallis region. North is toward the top; sunlight comes from southwest. See Figure 6 for location. (a) E11_01550: the floor of the crater lies at −3150 m, and the rim lies at −3050 m. (b) R06_00053: the floor of the crater lies at −2400 m, and the rim lies at −2250 m.

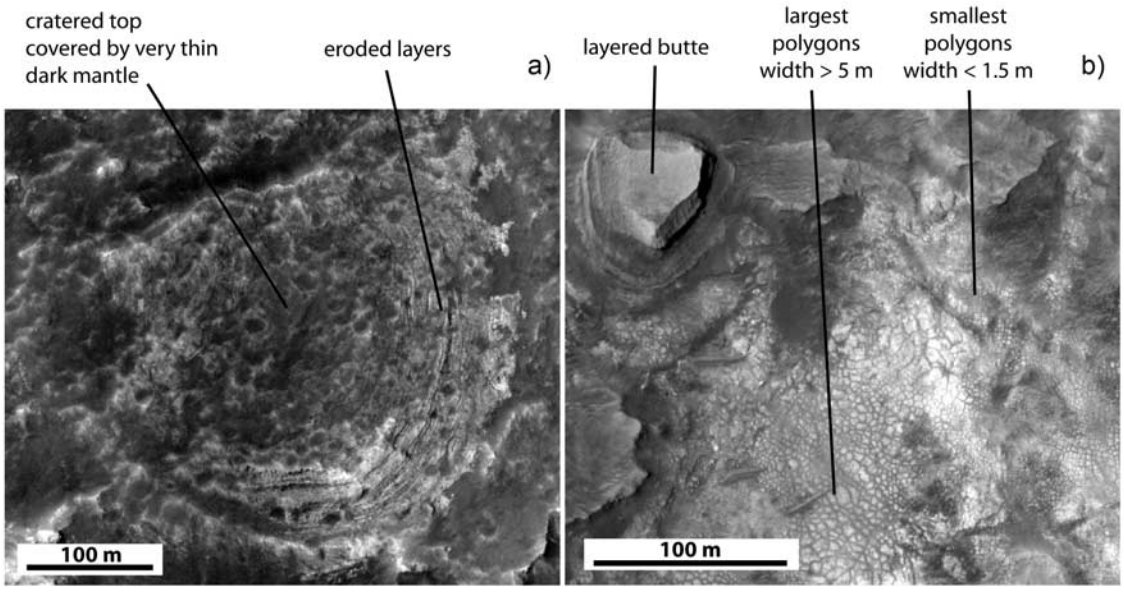

Figure 11. Two HiRISE close-ups on the plateau south of Mawrth Vallis mouth (see Figure 6 for location). North is at the top; light comes from west. (left) Three hundred meter large layered butte, dark and cratered at the top, with eroded layered wall. (right) White material heavily fractured by polygonal structures, covered in part by dunes, and by remains of dark mantle.

images display relatively cold temperatures: something on the surface lowers the thermal inertia. Two main hypotheses could explain this lack of hydrous minerals signature: (1) a process of dehydration or (2) a light dust mantling. The lower thermal inertia (as deduced by the lower temperature on THEMIS IR nighttime data) of these bright surfaces is more consistent with the second hypothesis, a light dust cover. Indeed, erosion of the phyllosilicate-rich layers could increase the surface dehydration rate, and lead to a surface residual lag devoid of hydration, which then would not show infrared signatures [e.g., *Cooper and Mustard*, 1999]. Alternatively, these zones could be composed of an unidentified material different from phyllosilicates that indicates a lateral change in the composition of the Noachian crust, but note that no mafic signatures have been detected on the bright unit using OMEGA data.

4.3. Relationships Between Phyllosilicates and Fluvial Landforms

[34] Two types of fluvial landforms that are related to two different timescales are observed in the region: the outflow channel of Mawrth Vallis and small valleys on the Noachian plateaus.

[35] The Mawrth Vallis outflow is a primitive outflow (dated to the late Noachian or early Hesperian [*Scott and Tanaka*, 1986]) for which the environment of formation is unknown, only requiring catastrophic water discharge for short durations, a few days or weeks [e.g., *Baker and Milton*, 1974; *Carr*, 1996] (whereas dendritic valleys might have formed over longer periods [e.g., *Carr*, 1996]). Several single, unconnected small valleys are visible on each side of Mawrth Vallis, cutting the phyllosilicate-rich unit, with most of them ending in Mawrth Vallis, hence postdating the formation of the outflow channel (Figure 13). On the other hand, a developed valley network with connections typical of dendritic networks is visible on the northeastern side of Mawrth Vallis mouth (Figure 14). It is discussed later in this section, along with Figure 14.

[36] Phyllosilicates are present on the sides of the Mawrth Vallis outflow channel and they have been detected locally on one large outcrop on its floor, located around −3300 m in altitude, named outcrop B (Figure 12). Figure 12 also shows that the bright unit seen on Mawrth Vallis floor and flanks is composed of thin layers locally exhumed as on the top of the cratered plateaus. Several streamlined islands (mapped on the context map, Figure 3) are composed of bright material with the most eroded outcrops displaying phyllosilicates signatures on OMEGA data. Streamlined islands in braided channels can correspond to material deposited by the channel and cut by later fluvial episodes or erosion of the underlying bedrock. From their rough morphology, these islands rather seem to correspond to bedrock erosion features as on most Martian outflow channels [*Baker and Milton*, 1974]. As phyllosilicates are also present high on the sides of the Mawrth Vallis, and as the bright floor of the channel locally shows erosional grooves, it is more likely that these phyllosilicate-rich outcrops correspond to an erosion of the underlying crust by the outflow incision. The presence of phyllosilicates in the middle of the outflow is thus not an exception to the interpretation of phyllosilicates being present in the highland bedrock. We nevertheless do not exclude local redeposition of phyllosilicates on the channel floor after the fluvial episode.

[37] A few branching valleys forming a small network are especially observed northeast of the outflow channel (Figure 14). They have a geometry very different to the outflow channel and they are more branched than the small ancient gullies cutting the Mawrth Vallis outflow sides. It is difficult to say if they are older or younger than the Mawrth Vallis channel because of their particular situation on the

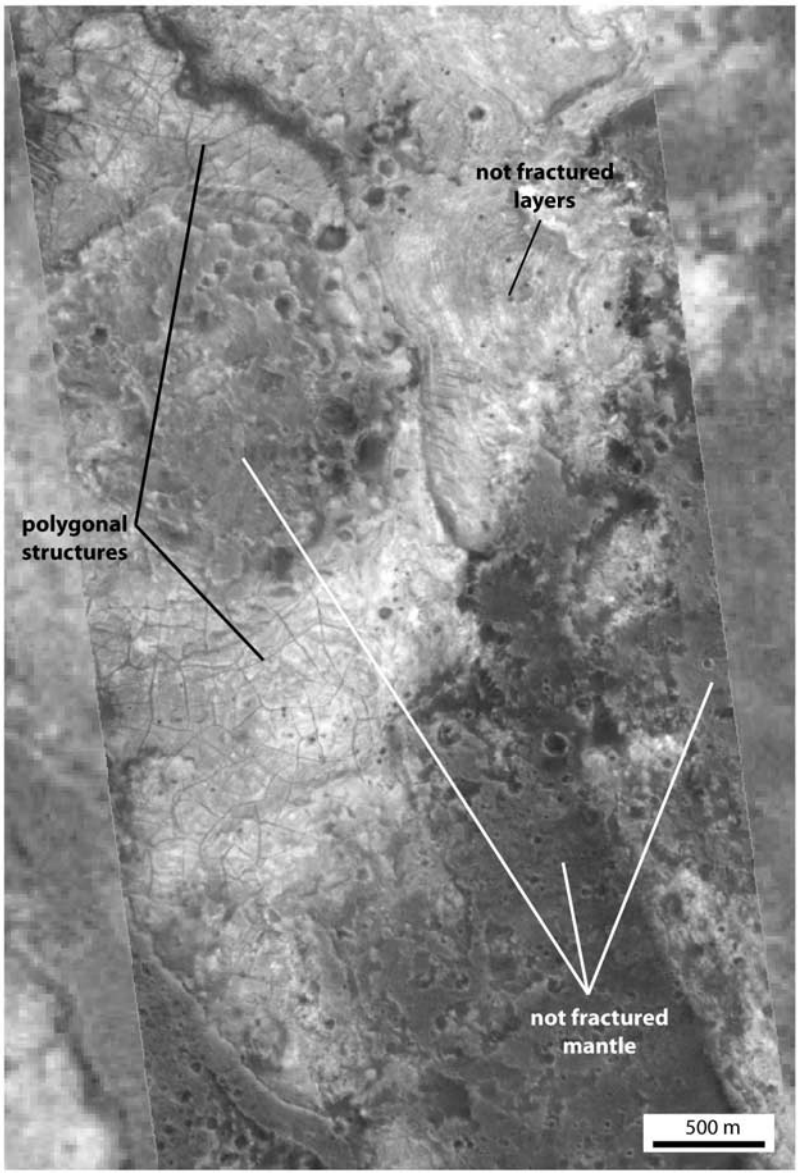

Figure 12. MOC image superimposed on HRSC image of polygonal structures on the floor of Mawrth Vallis (M18_00673; north is toward the top, and sunlight comes from the west; see Figure 6 for location).

lowlands northeast of Mawrth Vallis mouth: the lack of stratigraphic correlation with the outflow limits the interpretation of its age. It might be a Noachian age valley networks as those found usually in the Noachian bedrock [e.g., *Carr*, 1996]. As on the rest of the Noachian plateaus, the phyllosilicate signature appears in this area only on the brighter outcrops, which have medium temperature on THEMIS IR nighttime imagery. The ancient valleys are filled by dark material. The valleys seem to cut the phyllosilicate-rich unit, and hence formed after the formation of the bright unit. The western part of several valleys is topographically inverted (Figure 14, close-up A); the erosion preserved the valley material whereas the surrounding material has been exhumed. Many examples of valley inversion have been seen in other regions on Mars [e.g., *Malin and Edgett*, 2003; *Williams*, 2007]. This effect is especially important when the valley floor is filled by sand-gravel material, either as alluvial deposits during water flows or later by aeolian sand deposition. Indurated sand might be more resistant to wind erosion than indurated clay-size material, easily removable by wind. Here, the phyllosilicate-rich unit in which valleys formed underwent differential erosion: this unit is then probably composed of finer grain clay size material. The valley in the eastern part has a depth of about 50 meters showing that the erosion of the crust reached this value at minimum.

[38] In summary, the bright phyllosilicate-rich unit formed before the Mawrth Vallis outflow channel. Some later remobilization by flows or wind and downward deposition of material is possible. The relationship between the phyllosilicates and dendritic valleys has three interesting points: (1) the dendritic valleys are incised into the phyllo-

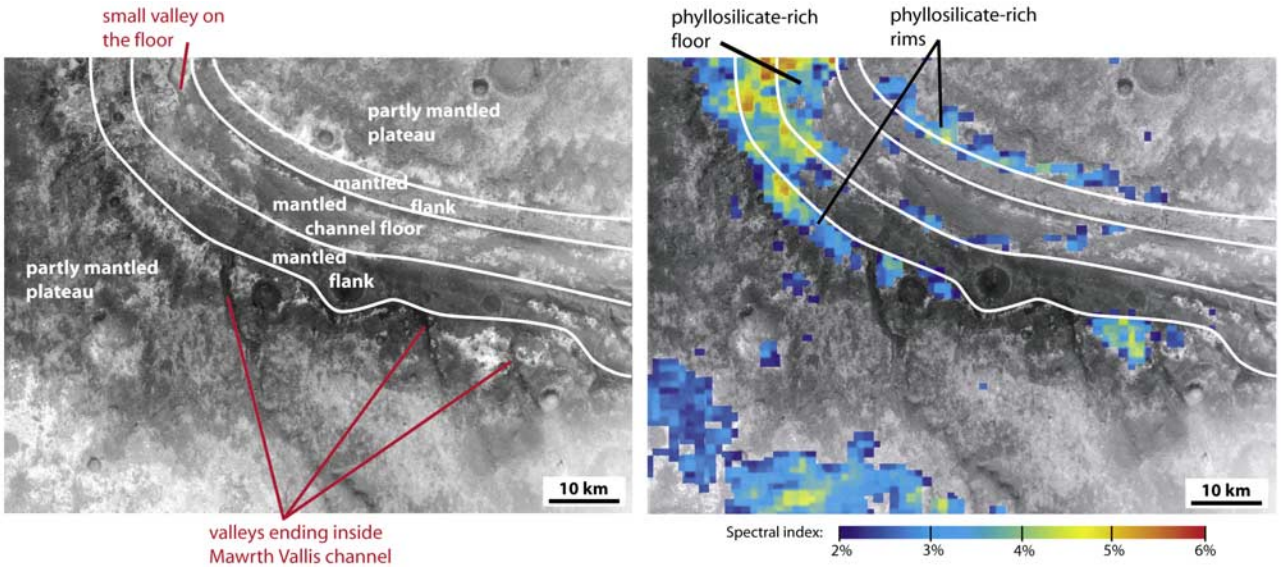

Figure 13. HRSC image with OMEGA spectral index of the 1.93 μm band. In red are indicated the valleys posterior to the formation of Mawrth Vallis (see Figure 6 for location and scale).

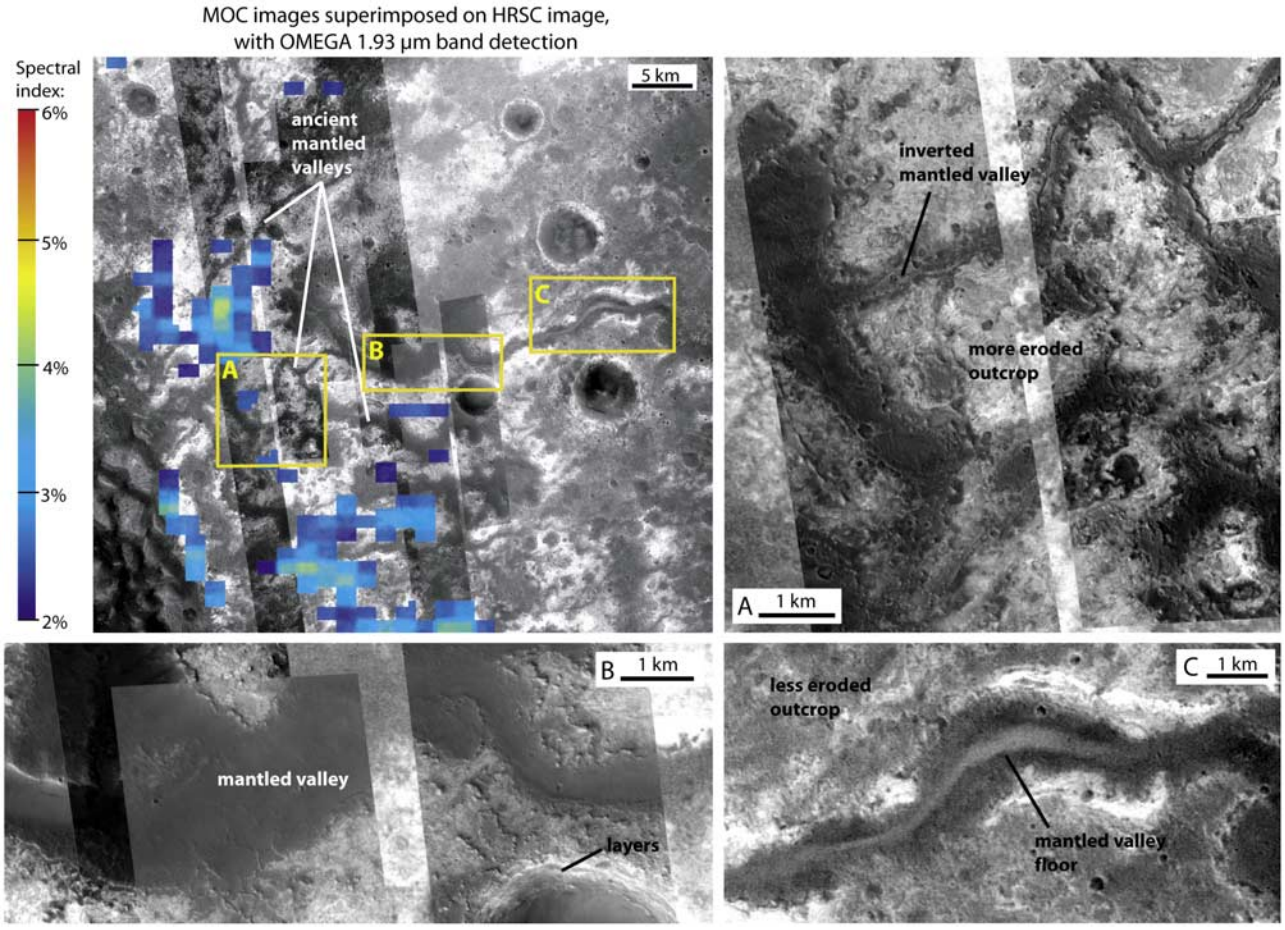

Figure 14. Detection of phyllosilicates in the vicinity of a valley network, east side of Mawrth Vallis mouth (see Figure 6 for location). (top left) HRSC image with superimposed MOC images and OMEGA spectral index of the 1.93 μm band. The regional slope goes from east to west. The yellow boxes indicate the locations of close-ups A, B, and C, which show terrains at different stages of erosion.

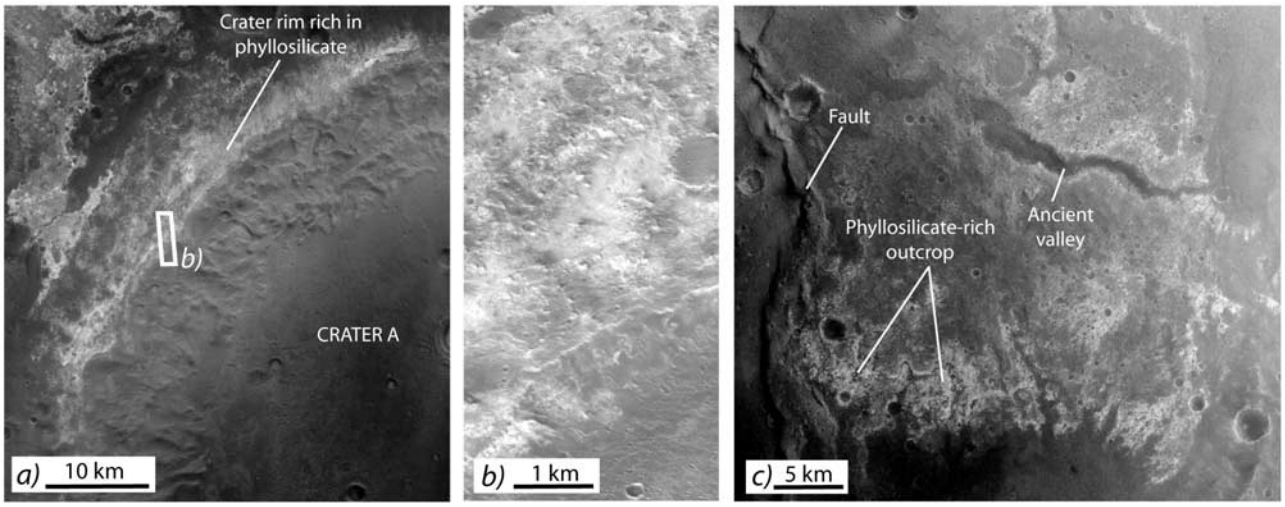

Figure 15. (a) HRSC close-up on the northwest corner of crater A (see Figure 6 for location). The brighter terrain on the rim and on the plateau toward the northwest is rich in phyllosilicates. The white box indicates the location of the MOC image in Figure 15b. (b) MOC narrow angle image M10-01551. North is toward the top; sunlight comes from the south. (c) HRSC close-up on the floor of crater A. The fault that crosses the crater is visible on the western side of the image, while an ancient valley lies on the north. OMEGA has detected phyllosilicates on the bright outcrop indicated in the southwest (see Figure 6 for location).

silicate-rich outcrops, (2) the amount of erosion of the Noachian bedrock at this location is at least 50 meters, and (3) the bright unit composed of phyllosilicates is easily eroded by wind as expected for clay-rich rocks with particle size <10 microns.

4.4. Relations of Phyllosilicates to Large Impact Craters

[39] The layered unit that contains phyllosilicates is clearly dated of Noachian age, but one can wonder if the formation of this unit preceded, was contemporaneous with, or postdated the formation of the large craters seen in the Mawrth Vallis region. When studying crater A, indicated in Figure 3, the 1.93 and 2.30 μm hydration bands appear on the northwest rim of the crater, at the highest point of the rim (Figures 15a and 15b). So it looks like the rocks rich in phyllosilicates that we see on the rim and the flanks of crater A were already formed at the time of the impact, and then at least a part of the phyllosilicate-rich unit was already deposited there at that time. Nevertheless, on the floor of the same crater, a bright outcrop can be seen (Figure 15c): OMEGA reveals Fe-OH smectite minerals on the western part which has been actively eroded. This small outcrop could be interpreted as either (1) a late phyllosilicate-rich area produced in the continuation of the phase that produced phyllosilicates in the basement, but with less intensity or (2) an erosion, transport and redeposition of rim material on the crater floor by erosion (aeolian or fluvial) processes. Also notice that small valleys, filled by dark material, cut this bright outcrop, indicating that small fluvial episodes happened after the impact. These observations still suggest that most of the phyllosilicate deposition/formation predates the formation of most of the major craters of the region, thus corresponding to a very primitive crust, with little phyllosilicate formed after, either as a residual activity or as remobilization of older ones.

4.5. Thickness of the Layered Unit

[40] One of the goals of these observations is to provide an estimate of the minimum thickness of the light toned layered unit in which we find phyllosilicates. Here, we do not focus only on exact locations where OMEGA found phyllosilicates, but on the geologic unit in which they are found as a whole. In a few places, residual buttes are large enough to show layers on their sides and to give an idea of the minimum thickness of this unit at that place. Figure 8b particularly gives an estimate of the thickness of a few tens of meters, based on the observation of the shadow of the butte. A more precise estimate can be made using the superimposition of MOLA topography over a MOC mosaic: Figure 9 shows heavily eroded terrain where layers are seen at different altitudes (the location is indicated in Figure 6). The topography of the outcrop indicates a unit at least 150 m thick. Another method for a local estimate of the thickness of the layered unit is the observation of layered crater walls around the craters of the region when they have the right dimensions, age, and erosion. Two examples are shown in Figure 10, where the eroded crater walls show layers along the whole perimeter. The MOLA topography leads to an estimate of 100 m of thickness in case a, Figure 10a, and up to 150 m in case b, Figure 10b. Moreover, as we have seen in Figure 14, the erosion of the valleys with inverted channels suggests a thickness of material that was once at least 50 m. In summary, the bright unit is layered over 100 meters at least in many locations.

[41] Locally, the polygonal structures seen on outcrop B on the floor of Mawrth Vallis can also provide an estimation of the thickness of the unit at this place. Mechanical studies made by *Parker* [1999] have shown that the depth of the material in which the contraction polygons are observed is at least a third of the minimal width of the polygons whatever their formation mechanism. With polygons typi-

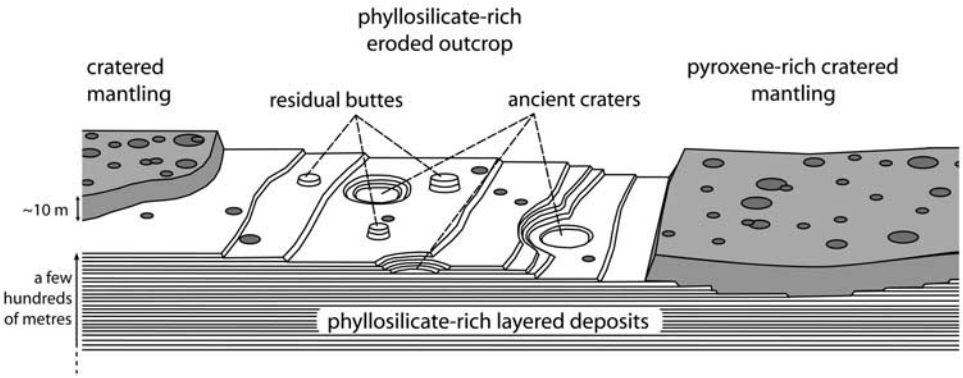

Figure 16. Schematic sketch of an example of an eroded outcrop of the phyllosilicate-rich unit of the Mawrth Vallis region.

cally 100 to 200 m in width, this would indicate a unit fractured over at least 30 m in depth, not excluding that the thickness is higher because the propagation of crack will be limited by thermal waves if due to seasonal temperatures variations. However, this place being at the bottom of the Mawrth Vallis channel, the phyllosilicate we observe there could have a different formation than the layered unit of the Noachian plateaus.

[42] As an illustration, in Figure 16, a schematic sketch shows how the cratered terrain may be. A bright phyllosilicate-rich layered unit appears on some outcrops. This bright unit may be several tens or hundreds of meters thick, and is partly covered by a dark pyroxene-rich mantle. Some residual buttes are present on the outcrops, with a few small craters generally filled by dark material. The dark mantle is estimated of the order of 10 m thick at a most, and usually covered by small craters. It appears that the old rocks have been exhumed from beneath a mantling unit that partly protected the underlying levels from the most recent small craters. During the exhumation, significant mechanical erosion has also been able to erase the smallest craters of the layered unit.

5. Discussion

5.1. Phyllosilicate-Rich Unit: A Thick Unit Rather Than a Thin Alteration Horizon

[43] Phyllosilicates often form on Earth as coatings and alteration horizons due to alteration of rocks on the surface and in microcracks, i.e., lava flows exposed to atmosphere and weathered to a few centimeters depth, rather than massively over a tens of meters thick unit [e.g., *Righi and Meunier*, 1995]. However, the thin alteration horizon hypothesis is difficult to reconcile with most observations. The presence of residual buttes, etched terrains and the lack of abundant small craters on the phyllosilicate-rich outcrops indicate that these outcrops are very eroded and recently exposed (i.e., several My). Thus, if the phyllosilicates were present as a thin horizon only, they would (1) have formed very quickly in the recent period or (2) be restricted to the uppermost part of layers of the Noachian bedrock. The first proposition is implausible because the formation of large amount of phyllosilicates under current atmospheric conditions is unlikely [*Gooding*, 1978; *Gooding et al.*, 1992] and the overall observation of phyllosilicates in Noachian rocks only [*Poulet et al.*, 2005] disfavors a recent formation. The second proposition is also unlikely because phyllosilicates are not restricted to a possible uppermost surface of the layered unit that would correspond to a residue of an old altered surface. On the contrary, phyllosilicates are better observed in the well exhumed material (e.g., Figure 7 and Figure 14). The interpretation of phyllosilicates as present over the whole unit also explains the lack of phyllosilicates outside the bright layered unit.

[44] The exact geometry of the phyllosilicate-rich unit is still unknown. Figure 17 shows two possible representations of the unit assuming a horizontal geometry or tilted beds. If we assume that the layers are horizontal and that the phyllosilicate is intrinsic to the bedrock lithology, the phyllosilicate being detected at altitudes going from −3650 m (north of Mawrth Vallis mouth) to −1650 m (south of the channel), it would suggest that the unit could reach 2000 m in thickness (Figure 17, top sketch). This thickness is likely overestimated due to the regional deformation: the unit could be a pre-dichotomy unit tilted and slightly deformed by the dichotomy formation and by large impact craters (Figure 17, bottom sketch). In that case, the layers of the unit could follow more or less the long wave topography, and the thickness would not exceed a few hundred meters. The meter-scale layers of the phyllosilicate-rich unit cannot be seen on HRSC data; only MOC and HiRISE imagery reach a sufficient resolution. At such a small scale, and using only MOLA topography, it is not possible to retrieve dips for the layers we see. However, future work involving HRSC digital terrain models could help us in understanding the geometry of the unit. Nevertheless, notice that layers are observed on nearby outcrops both near the floor of Mawrth Vallis (Figure 12) and on the Noachian plateaus, with more than 500 m of difference in elevation locally (Figure 17, bottom). This geometry would indicate that the outflow channel incised 500 m of layered unit. Besides, note that we observed no indication of basement beneath the bright layered unit in the whole area.

5.2. Implications for the Past Environment

[45] The smectites detected by OMEGA, similar to nontronite and montmorillonites, are the constituents of clay-rich altered rocks on Earth. The presence of smectites is a

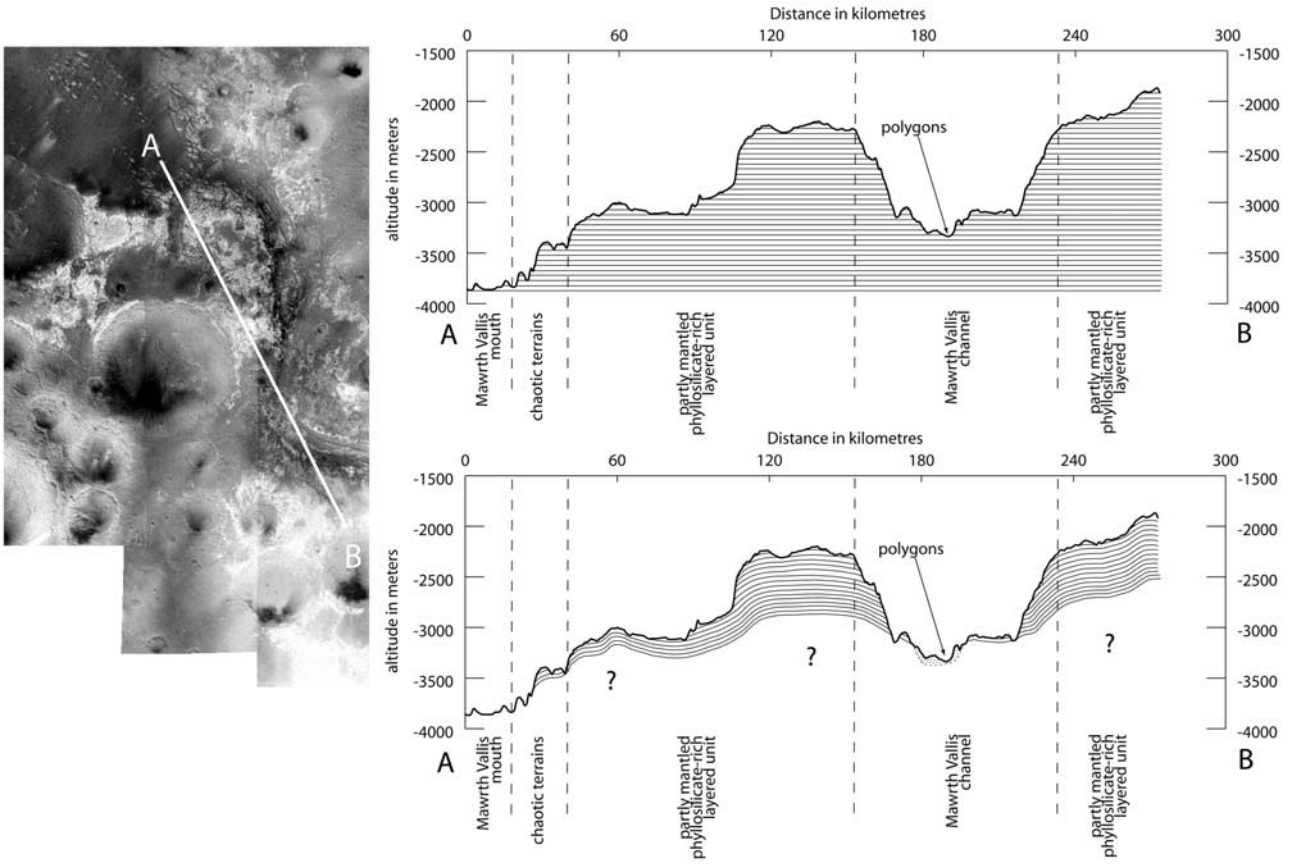

Figure 17. Two different schematic possible representations of the layered unit of the region of Mawrth Vallis. The top sketch shows a unit that did not move since its formation. The bottom sketch shows a strongly modified unit. An intermediate hypothesis would show layers with a dip similar to the regional slope, provoked by the formation of the dichotomy.

strong indicator of the occurrence of low-temperature alteration (lower than 500°C [e.g., *Güven*, 1988]) which on Earth are the result of the alteration of igneous rocks by liquid water over long periods of time [*Gislason and Arnorsson*, 1993; *Velde*, 1995]. The minimum thickness of 150 m and the geographic extension over more than 400 km × 300 km indicates that the process of formation of these phyllosilicates was widespread in the region, excluding local hydrothermalism. Hence, if the processes of alteration of rocks into phyllosilicates are the same on Mars as on Earth, then the presence of phyllosilicates in the Mawrth Vallis region indicates a formational environment very different from the current surface environment. The presence of smectite clay minerals also indicates an aqueous environment that was more neutral to alkaline than for the formation of sulfate-rich rocks [*Poulet et al.*, 2005; *Bibring et al.*, 2006].

[46] Hypotheses of formation include (1) siliciclastic sediments deposited by water in an aqueous environment very early in the Mars history, probably before the dichotomy; (2) strong alteration by liquid water of volcanic ash deposits, or of a wind-blown deposited unit, draping the primitive crust; (3) deposition of a phyllosilicate-rich aeolian unit; (4) accumulation of altered ejecta from the large impacts during the heavy bombardment; and (5) strong in situ alteration by liquid water of primitive lava flows.

[47] The presence of phyllosilicates in outcrops of a thick unit composed of thin and regular meter scale layers, the medium thermal inertia and mechanical properties of these layers, and the lack of mafic signatures favor the presence of clays in thin sedimentary layers. In the first hypothesis, the sediments might involve an aqueous process in which clays are part of a system of alteration, transportation and deposition. These deposits would be supposed to be in a basin, whereas in the Mawrth Vallis region, with the current topography, we observe layers at the summit of the Noachian plateaus. Nevertheless, the topography of the primitive epoch, before the dichotomy, is not known, and could have been modified intensively since the deposition, as illustrated in Figure 17 (bottom figure). Moreover the elevation at −3300 m is rather an argument consistent with the possibility of an old accumulation basin at that place. This hypothesis suggests the phyllosilicate-rich unit to be similar to shales, or argillite, found on Earth.

[48] In the second case, the alteration take place after the accumulation of material from atmospheric deposition, and water is involved close to the surface or in the subsurface in aquifers. The alteration of volcanic grains of ash or wind-blown material should have been very strong to remove any other signatures such as pyroxenes from these deposits. This process should have formed phyllosilicates close to surface but the relatively cold temperature would have required a

long duration at low alteration rates. If such alteration occurred through hydrothermalism, the process was unlikely to have been local because of the geographic extent of the unit. The unusually high thermal gradient in the Noachian period [e.g., *Schubert et al.*, 1992] might then be a possibility for strong alteration at relatively higher rates than at the surface.

[49] In the third hypothesis, the accumulation would have come from a material that would have already been altered into clays. In that case, the origin of the alteration would remain unknown. We do not favor this hypothesis because such an accumulation would require a large source of altered rocks and a particular atmospheric dynamics, though no other clay outcrops has been identified in the vicinity yet.

[50] The fourth hypothesis, a continuous layer of ejecta blankets, is difficult to reconcile with the geographic extent of the unit, but the effect of heavy bombardment on a water-rich crust could have been important [e.g., *Newsom*, 1980]. The observations of hydrated ejecta in the Nili Fossae region [*Mangold et al.*, 2007] and in Terra Thyrrhena [*Poulet et al.*, 2006] do not favor this possibility in our case: in the Nili Fossae region, eroded ejecta with hydrated minerals display textures with fluidization patterns, lack of regular and thin layers, and the presence of boulders inside the material. We did not find any of these characteristics in the thin layers of the light-toned unit of the Mawrth Vallis region. Thus only a contribution of impact processes is possible, either to the accumulation of material, or to the heat of crustal rocks to increase the alteration kinetics.

[51] The fifth hypothesis is similar to the second one, but for the alteration of lava flows. At the difference of ash or wind-blown material, lava flows are usually thick ($\sim$10 m layers as seen in Valles Marineris flanks) with rather higher thermal inertia. No mafic minerals have been detected with OMEGA, even as a residue or mixed with phyllosilicates. This possibility seems very unlikely from these arguments.

[52] Comparisons with other regions are also crucial for a global understanding. In the Nili Fossae region [*Mangold et al.*, 2007], phyllosilicates are found on more diverse types of rocks (layered units, massive units, crater ejecta, and dyke-rich rocks in association with olivine-rich unit). The Mawrth Vallis region displays only one type of geologic context for the phyllosilicate-rich rocks (and the bright outcrop in crater A, and outcrop B at the bottom of Mawrth Vallis, could possibly be exceptions): a bright layered unit, through the different examples of rocks observed; we are thus unsure whether these rocks are the most common type of altered rocks in the Noachian crust, but it suggests more superficial alteration than in Nili Fossae where hydrothermalism may explain most signatures [*Mangold et al.*, 2007].

[53] The fact that the rocks are very old makes uncertain the preservation of criteria that would have permitted the discrimination of these hypotheses from orbital data. To know if the accumulation occurred mainly at surface or subsurface, we would need to know the depth at which it occurred, something difficult to estimate as it depends on the amount of exhumation: whether the current surface is close to the original one.

6. Conclusion

[54] The OMEGA spectrometer onboard Mars Express provides unique detections of hydrous minerals which consist of Al- and Mg- or Fe-OH smectites in the Mawrth Vallis region. The correlation of these mineralogical signatures and the geologic and physical properties from HRSC, THEMIS, MOC and HiRISE data lead to the following conclusions:

[55] 1. Phyllosilicates are associated with bright outcrops of the Noachian crust only, covering many outcrops over a 300 $\times$ 400 km region.

[56] 2. No mafic minerals are detected in combination with phyllosilicates anywhere. Pyroxene is found at the mouth of Mawrth Vallis, probably as a filling by Acidalia lava plains, and as a constituent of aeolian material such as dark dunes inside craters, or in the mantling on top of the Noachian plateaus. This pyroxene-rich mantling overlies the phyllosilicate-rich unit and is geologically younger.

[57] 3. The bright phyllosilicate-rich unit is highly eroded and displays a minimum thickness of 150 m with layering at the meter scale.

[58] 4. The phyllosilicate-rich unit has the geological, physical and mineralogical characteristics of shales, or argillites, formed by the deposition and induration of clay-size material.

[59] 5. The different hypotheses of formation of this phyllosilicate-rich unit include (1) sediments deposited by water in an aqueous environment (i.e., deposition of transported phyllosilicates) and (2) alteration by liquid water of volcanic ash deposits, or other wind deposited unit, to produce in situ phyllosilicates. A contribution of phyllosilicate-rich wind-blown material is possible but this process might better explain more recent redeposition such as in crater A. A contribution of craters ejecta during the heavy bombardment is an alternative process, but seems less likely based on the phyllosilicate-rich unit extent and characteristics.

[60] 6. Chronological relationships with other units and large craters show that this phyllosilicate-rich unit formed early in the history, possibly before the dichotomy formation. The chronological relationships with fluvial features show that the observed aqueous flows occurred after the formation of the phyllosilicate-rich unit, without being involved in its formation, with exception of redeposition of materials in low lying areas.

[61] Quantifying the proportion of minerals and observing the sedimentary facies of the bright phyllosilicate-rich layers using in situ rovers would certainly improve the understanding of these rocks that are key features for the reconstruction of the early Mars environment.

[62] **Acknowledgments.** We thank the HRSC Experiment Teams at DLR Berlin and Freie Universität Berlin as well as the Mars Express Project Teams at ESTEC and ESOC for their successful planning and acquisition of data as well as for making the processed data available to the HRSC Team. We acknowledge the effort of the OMEGA and HRSC Co-Investigator Team members and their associates who have contributed to this investigation in the preparatory phase and in scientific discussions within the teams, and particularly Greg Michael for his careful reading of the manuscript. We acknowledge the MOC/MGS, THEMIS/Mars Odyssey, and HiRISE/MRO teams for the use of their data available on the respective Web sites: http://www.msss.com/moc_gallery/, http://themis.asu.edu/, and http://marsoweb.nas.nasa.gov/HiRISE/. Careful and constructive reviews by M. S. Lane and T. D. Glotch helped to significantly improve the manuscript. The authors are granted by the Centre National d'Etudes Spatiales (CNES) and the Programme National de Planétologie (PNP) of Institut National des Sciences de l'Univers (INSU).

References

Baker, V. R., and D. J. Milton (1974), Erosion by catastrophic floods on Mars and Earth, *Icarus*, *23*, 27–41.

Bibring, J.-P., et al. (2004), OMEGA: Observatoire pour la Minéralogie, l'Eau, les Glaces et l'Activité, in *Mars Express: The Scientific Payload*, edited by A. Wilson, *Eur. Space Agency Spec. Publ.*, *ESA-SP 1240*, 37–49.

Bibring, J.-P., et al. (2005), Mars surface diversity as revealed by the OMEGA/Mars Express observations, *Science*, *307*, 1576–1581.

Bibring, J.-P., Y. Langevin, J. F. Mustard, F. Poulet, R. Arvidson, A. Gendrin, B. Gondet, N. Mangold, P. Pinet, and F. Forget (2006), Global mineralogical and aqueous Mars history derived from the OMEGA/Mars Express data, *Science*, *312*, 400–404.

Carr, M. H. (1996), Channels and valleys on Mars: Cold climate features formed as a result of a thickening cryosphere, *Planet. Space Sci.*, *44*, 1411–1423.

Christensen, P. R., et al. (2001), Mars Global Surveyor Thermal Emission Spectrometer experiment: Investigation description and surface science results, *J. Geophys. Res.*, *106*(E10), 23,823–23,872.

Christensen, P. R., et al. (2003), Morphology and composition of the surface of Mars: Mars Odyssey THEMIS results, *Science*, *300*(5628), 2056–2061, doi:10.1126/science.1080885.

Christensen, P. R., et al. (2004), The Thermal Emission Imaging System (THEMIS) for the Mars 2001 Odyssey mission, *Space Sci. Rev.*, *110*(1), 85–130, doi:10.1023/B:SPAC.0000021008.16305.94.

Clark, R. N., T. V. V. King, M. Klejwa, G. A. Swayze, and N. Vergo (1990), High spectral resolution reflectance spectroscopy of minerals, *J. Geophys. Res.*, *95*(B8), 12,653–12,680.

Clark, R. N., G. A. Swayze, A. Gallagher, T. V. V. King, and W. M. Calvin (1993), The USGS Digital Spectral Library: Version 1: 0.2 to 3.0 microns, *U.S. Geol. Surv. Open File Rep.*, *93-592*, 1340 pp. (Available at http://speclab.cr.usgs.gov)

Cooper, C. D., and J. F. Mustard (1999), Effects of very fine particle size on reflectance spectra of smectite and palagonitic soil, *Icarus*, *142*, 557–570, doi:10.1006/icar.1999.6221.

Edgett, K. S. (2002), Low-albedo surfaces and eolian sediment: Mars Orbiter Camera views of western Arabia Terra craters and wind streaks, *J. Geophys. Res.*, *107*(E6), 5038, doi:10.1029/2001JE001587.

Edgett, K. S., and M. C. Malin (2002), Martian sedimentary rock stratigraphy: Outcrops and interbedded craters of northwest Sinus Meridiani and southwest Arabia Terra, *Geophys. Res. Lett.*, *29*(24), 2179, doi:10.1029/2002GL016515.

Edgett, K. S., and T. J. Parker (1997), Water on early Mars: Possible subaqueous sedimentary deposits covering ancient cratered terrain in western Arabia and Sinus Meridiani, *Geophys. Res. Lett.*, *24*(22), 2897–2900.

Gislason, S. R., and S. Arnorsson (1993), Dissolution of primary basaltic minerals in natural waters: Saturation state and kinetics, *Chem. Geol.*, *105*, 117–135.

Gooding, J. L. (1978), Chemical weathering on Mars—Thermodynamic stabilities of primary minerals and their alteration products from mafic igneous rocks, *Icarus*, *33*, 483–513, doi:10.1016/0019-1035(78)90186-0.

Gooding, J. L., R. E. Arvidson, and M. Y. Zolotov (1992), Physical and chemical weathering, in *Mars*, edited by H. H. Kieffer et al., pp. 626–651, Univ. of Ariz. Press, Tucson.

Güven, N. (1988), Smectite, in *Hydrous Phyllosilicates*, *Rev. Mineral.*, vol. 19, edited by S. W. Bailey, pp. 497–522, Mineral. Soc. of Am., Washington, D. C.

Malin, M. C., and K. S. Edgett (2000), Sedimentary rocks of early Mars, *Science*, *290*(5498), 1927–1937.

Malin, M. C., and K. S. Edgett (2003), Evidence for persistent flow and aqueous sedimentation on early Mars, *Science*, *302*(5652), 1931–1934, doi:10.1126/science.1090544.

Malin, M. C., G. E. Danielson, A. P. Ingersoll, H. Masursky, J. Veverka, M. A. Ravine, and T. A. Soulanille (1992), Mars Observer Camera, *J. Geophys. Res.*, *97*(E5), 7699–7718.

Mangold, N. (2005), High latitude patterned grounds on Mars: Classification, distribution and climatic control, *Icarus*, *174*(2), 336–359, doi:10.1016/j.icarus.2004.07.030.

Mangold, N., et al. (2007), Mineralogy of the Nili Fossae region with OMEGA/Mars Express data: 2. Aqueous alteration of the crust, *J. Geophys. Res.*, doi:10.1029/2006JE002835, in press.

McEwen, A. S., et al. (2007), Mars Reconnaissance Orbiter's High Resolution Imaging Science Experiment (HiRISE), *J. Geophys. Res.*, *112*, E05S02, doi:10.1029/2005JE002605.

Mellon, M. T., B. M. Jakosky, H. H. Kieffer, and P. R. Christensen (2000), High-resolution thermal inertia mapping from the Mars Global Surveyor Thermal Emission Spectrometer, *Icarus*, *148*(2), 437–455, doi:10.1006/icar.2000.6503.

Mustard, J. F., F. Poulet, A. Gendrin, J.-P. Bibring, Y. Langevin, B. Gondet, N. Mangold, G. Bellucci, and F. Altieri (2005), Olivine and pyroxene diversity in the crust of Mars, *Science*, *307*(5715), 1594–1597, doi:10.1126/science.1109098.

Neukum, G., and R. Jaumann (2004), HRSC: The High Resolution Stereo Camera of Mars Express, in *Mars Express: The Scientific Payload*, edited by A. Wilson, *Eur. Space Agency Spec. Publ.*, *ESA-SP 1240*, 17–35.

Newsom, H. E. (1980), Hydrothermal alteration of impact melt sheets with implications for Mars, *Icarus*, *44*, 207–216, doi:10.1016/0019-1035(80)90066-4.

Parker, A. P. (1999), Stability of arrays of multiple edge cracks, *Eng. Fracture Mech.*, *62*, 577–591.

Pelkey, S. M., B. M. Jakosky, and M. T. Mellon (2001), Thermal inertia of crater-related wind streaks on Mars, *J. Geophys. Res.*, *106*(E10), 23,909–23,920.

Pelkey, S. M., B. M. Jakosky, and P. R. Christensen (2003), Surficial properties in Melas Chasma, Mars, from Mars Odyssey THEMIS data, *Icarus*, *165*(1), 68–89.

Poulet, F., N. Mangold, and S. Erard (2003), A new view of dark Martian regions from geomorphic and spectrocopic analysis of Syrtis Major, *Astron. Astrophys.*, *412*, L19–L23, doi:10.1051/0004-6361:20031661.

Poulet, F., J.-P. Bibring, J. F. Mustard, A. Gendrin, N. Mangold, Y. Langevin, R. E. Arvidson, B. Gondet, and C. Gomez (2005), Phyllosilicates on Mars and implications for early Martian climate, *Nature*, *438*(7068), 623–627, doi:10.1038/nature04274.

Poulet, F., J.-P. Bibring, Y. Langevin, B. Gondet, J. Mustard, A. Gendrin, N. Mangold, D. Loizeau, R. E. Arvidson, and V. Chevrier (2006), The distribution of phyllosilicates on Mars from the OMEGA-MEx imaging spectrometer, *Proc. Lunar Planet. Sci. Conf. 37th*, Abstract 1698.

Poulet, F., C. Gomez, J.-P. Bibring, Y. Langevin, B. Gondet, P. Pinet, G. Belluci, and J. Mustard (2007), Martian surface mineralogy from Observatoire pour la Minéralogie, l'Eau, les Glaces et l'Activité on board the Mars Express spacecraft (OMEGA/MEx): Global mineral maps, *J. Geophys. Res.*, doi:10.1029/2006JE002840, in press.

Presley, M. A., and P. R. Christensen (1997), The effect of bulk density and particle size sorting on the thermal conductivity of particulate materials under Martian atmospheric pressures, *J. Geophys. Res.*, *102*(E4), 9221–9230.

Putzig, N. E., M. T. Mellon, K. A. Kretke, and R. E. Arvidson (2005), Global thermal inertia and surface properties of Mars from the MGS mapping mission, *Icarus*, *173*(2), 325–341, doi:10.1016/j.icarus.2004.08.017.

Righi, D., and A. Meunier (1995), Origin of clays by rock weathering and soil formation, in *Origin and Mineralogy of Clays*, edited by B. Velde, pp. 43–161, Springer, New York.

Rogers, A. D., and P. R. Christensen (2007), Surface mineralogy of Martian low-albedo regions from MGS-TES data: Implications for upper crustal evolution and surface alteration, *J. Geophys. Res.*, *112*, E01003, doi:10.1029/2006JE002727.

Schubert, G., S. C. Solomon, D. L. Turcotte, M. J. Drake, and N. H. Sleep (1992), Origin and thermal evolution of Mars, in *Mars*, edited by H. H. Kieffer et al., pp. 147–183, Univ. of Ariz. Press, Tucson.

Scott, D. H., and K. L. Tanaka (1986), Geologic map of western equatorial region of Mars, *U.S. Geol. Surv. Misc. Invest Ser.*, *Map I-1802-A*.

Smith, D. E., et al. (2001), Mars Orbiter Laser Altimeter: Experiment summary after the first year of global mapping of Mars, *J. Geophys. Res.*, *106*(E10), 23,689–23,722.

Velde, B. (1995), Composition and mineralogy of clay minerals, in *Origin and Mineralogy of Clays*, edited by B. Velde, pp. 8–42, Springer, New York.

Watters, T. R. (1993), Compressional tectonism on Mars, *J. Geophys. Res.*, *98*(E9), 17,049–17,060.

Williams, R. M. E. (2007), Global spatial distribution of raised curvilinear features on Mars, *Lunar Planet. Sci., XXXVIII*, Abstract 1821.

V. Ansan, D. Loizeau, N. Mangold, and P. Masson, Laboratoire IDES, Université Paris XI, Bâtiment 509, F-91405 Orsay, France. (damien.loizeau@u-psud.fr)

J.-P. Bibring, A. Gendrin, C. Gomez, B. Gondet, Y. Langevin, and F. Poulet, Institut d'Astrophysique Spatiale, Bâtiment 120, Université Paris XI, F-91405 Orsay, France.

G. Neukum, Institut für Geologische Wissenschaften, Freie Universität Berlin, D-12249 Berlin, Germany.